

1  
2

3

4

5

## The Virtual Space Weather Modelling Centre

6

7 Stefaan Poedts<sup>1,9\*</sup>, Andrey Kochanov<sup>1</sup>, Andrea Lani<sup>1</sup>, Camilla Scolini<sup>1,2</sup>, Christine Verbeke<sup>1</sup>,  
8 Skralan Hosteaux<sup>1</sup>, Emmanuel Chané<sup>1</sup>, Herman Deconinck<sup>3</sup>, Nicolae Mihalache<sup>4</sup>, Fabian  
9 Diet<sup>4</sup>, Daniel Heynderickx<sup>5</sup>, Johan De Keyser<sup>6</sup>, Erwin De Donder<sup>6</sup>, Norma B. Crosby<sup>6</sup>,  
10 Marius Echim<sup>6</sup>, Luciano Rodriguez<sup>2</sup>, Robbe Vansintjan<sup>2</sup>, Freek Verstringe<sup>2</sup>, Benjamin  
11 Mampaey<sup>2</sup>, Richard Horne<sup>7</sup>, Sarah Glauert<sup>7</sup>, Piers Jiggins<sup>8</sup>, Ralf Keil<sup>8</sup>, Alexi Glover<sup>8</sup>,  
12 Grégoire Deprez<sup>8</sup>, Juha-Pekka Luntama<sup>8</sup>

13

14 <sup>1</sup>KU Leuven, Leuven, Belgium

15 <sup>2</sup>Royal Observatory of Belgium, Ukkel, Belgium

16 <sup>3</sup>Von Karman Institute, Sint-Genesius-Rode, Belgium

17 <sup>4</sup>Space Applications Systems, Zaventem, Belgium

18 <sup>5</sup>DH Consultancy, Leuven, Belgium

19 <sup>6</sup>Royal Belgian Institute for Space Aeronomy, Ukkel, Belgium

20 <sup>7</sup>British Antarctic Survey, Cambridge, United Kingdom

21 <sup>8</sup>European Space Agency

22 <sup>9</sup>Institute of Physics, University of Maria Curie-Skłodowska, Lublin, Poland

23

24 [\\*Stefaan.Poedts@kuleuven.be](mailto:Stefaan.Poedts@kuleuven.be)

25

26 Short title (running head): Virtual Space Weather Modelling Centre

27

28

29 **Abstract**

30

31 **Aims**

32 Our goal is to develop and provide an open end-to-end (Sun to Earth) space weather  
33 modeling system, enabling to combine ("couple") various space weather models in an  
34 integrated tool, with the models located either locally or geographically distributed, so as to  
35 better understand the challenges in creating such an integrated environment.

36

37 **Methods**

38 The physics-based models are installed on different compute clusters and can be run  
39 interactively and remotely and that can be coupled over the internet, using open source  
40 'high-level architecture' software, to make complex modeling chains involving models from  
41 the Sun to the Earth. Visualization tools have been integrated as 'models' that can be coupled  
42 to any other integrated model with compatible output.

43

44 **Results**

45 The first operational version of the VSWMC is accessible via the SWE Portal and  
46 demonstrates its end-to-end simulation capability. Users interact via the front-end GUI and  
47 can interactively run complex coupled simulation models and view and retrieve the output,  
48 including standard visualizations, via the GUI. Hence, the VSWMC provides the capability  
49 to validate and compare model outputs.

50

51 **Table of contents:**

52 **1 INTRODUCTION.....3**

53 **2 GENERAL DESCRIPTION AND OBJECTIVE(S).....5**

54 2.1 Background .....5

55 2.2 Long term objective: future more advanced VSWMC.....6

56 2.3 Potential user groups/users.....7

57 2.4 Short term objective: VSWMC Part 2 .....7

58 2.5 Outcome .....7

59 **3 DESIGN OF THE FULL VSWMC SYSTEM..... 8**

60 3.1 Assets Review and Customer Requirements ..... 8

61 3.2 System requirements .....9

62 3.3 Architectural and detailed design .....10

63 **4 RELEASE OF THE VSWMC ..... 12**

64 4.1 Development of the VSWMC core system ..... 12

65 4.2 Interfacing of additional space weather models..... 12

66 4.3 Operational models..... 13

67 4.3.1 EUHFORIA-Corona ..... 14

68 4.3.2 EUHFORIA-Heliosphere ..... 15

69 4.3.3 GUMICS-4..... 17

70 4.3.4 BAS-RBM ..... 19

71 4.3.5 Kp prediction model.....25

72 4.3.6 Dst prediction model.....27

73 4.3.7 Magnetopause standoff distance model ..... 30

74 4.3.8 ODI .....32

75 4.3.9 Visualization ‘federate’ .....32

76 4.4 Development of Data provision nodes ..... 34

77 4.5 Running models and coupled models via the User Front-End (GUI) .....35

78 **5 FUNCTIONALITY OF THE SYSTEM .....39**

79 **6 LESSONS LEARNED AND FUTURE DEVELOPMENT ..... 40**

80 6.1 Challenges and lessons learned ..... 40

81 6.2 Future updates and development ..... 41

82 **7 SUMMARY AND CONCLUSION .....42**

83 **BIBLIOGRAPHY .....43**

84  
85

86 **1 INTRODUCTION**

87 Given the enormous socio-economic impact of space weather on Earth [Eastwood et al.,  
88 2017], it is increasingly important to provide reliable predictions of the space weather and  
89 its effects on our ground-based and space-borne technological systems, human life and  
90 health. This requires a deeper insight in the physical mechanisms that are causing the space  
91 weather and its multiple effects. Clearly, observations and continuous monitoring are also  
92 extremely important but sometimes observations are limited or difficult to interpret (due to  
93 e.g. projection effects) and some important parameters can simply not be observed directly

94 (e.g. the coronal magnetic field). In these cases we have to rely on mathematical models. As  
95 a matter of fact, such models can take into account the physical and/or chemical processes  
96 behind the phenomena of interest and the resulting equations can be solved by powerful  
97 computer clusters. Such numerical simulation models become ever more realistic and can  
98 provide additional information where direct observations are not possible, such as on the  
99 solar coronal magnetic field topology, the density structure in a CME or magnetic cloud, and  
100 the local velocity of an approaching CME. After appropriate validation, some of these models  
101 even have a predictive value so that they can be used for forecasting for instance the arrival  
102 of a CME shock at Earth or the radiation to be expected at the location of a satellite, enabling,  
103 in some cases, mitigation of its destructive effects.

104  
105 Empirical and semi-empirical models are much simpler and to be preferred for forecasting  
106 and predictions as long as they are reliable. When they are not working satisfactorily,  
107 physics-based models can bring a solution. However, such physics-based models are often  
108 rather complicated and difficult to install and operate. Moreover, they often require a  
109 substantial amount of CPU time and computer memory to run efficiently and they produce  
110 enormous amounts of output that needs to be interpreted, analysed and visualised.  
111 Therefore, integrated Space Weather model frameworks are being developed that provide a  
112 simple (graphical) user interface to simplify the use of such simulation models. The  
113 Community Coordinated Modeling Center (CCMC, <https://ccmc.gsfc.nasa.gov/>), for  
114 instance, is a multi-agency (NASA, NSF) initiative that “enables, supports and performs the  
115 research and development for next-generation space science and space weather models”.  
116 The Space Weather Modeling Framework (SWMF, Tóth et al. 2005) at the Center for Space  
117 Environment Modeling (CSEM) at the University of Michigan (USA) is another example of  
118 such a framework. CSEM too develops high-performance simulation models and uses them  
119 to forecast space weather and its effects. These frameworks thus provide a standard  
120 environment and serve as model and data repositories, enable model simulation runs and  
121 validation of the obtained results and even facilitate the coupling of different (sub) models  
122 integrated in the framework to support space weather forecasters and even space science  
123 education.

124  
125 The ESA Virtual Space Weather Modelling Centre (VSWMC) is an ambitious project that  
126 aims to develop an alternative European framework with extra features and facilities. The  
127 VSWMC-Part 2 project was part of the ESA Space Situational Awareness (SSA) Programme  
128 which is being implemented as an optional ESA programme supported by 19 Member States  
129 ([https://www.esa.int/Our\\_Activities/Space\\_Safety/SSA\\_Programme\\_overview](https://www.esa.int/Our_Activities/Space_Safety/SSA_Programme_overview)).  
130 More precisely, it was part of the Space Weather Segment (SWE) of the SSA Period 2  
131 programme as a ‘Targeted Development’, viz. P2-SWE-XIV: Virtual Space Weather  
132 Modelling Centre. This ambitious project further developed the VSWMC building on the Part  
133 1 prototype system that was developed as a GSTP (General Support Technology Programme)  
134 project (Contract No. 4000106155, ESTEC ITT AO/1-6738/11/NL/AT, 2012-2014), and  
135 focusing on the interaction with ESA’s SSA SWE system. This included the efficient  
136 integration of new models and new model couplings (compared to the earlier prototype),  
137 including a first demonstration of an end-to-end simulation capability, but also the further  
138 development and wider use of the coupling toolkit and the front-end GUI which was  
139 designed to be accessible via the SWE Portal (<http://swe.ssa.esa.int/>), and the addition of

140 more accessible input and output data on the system and development of integrated  
141 visualization tool modules.

142  
143 The consortium that took up this challenge consisted of KU Leuven (prime contractor,  
144 Belgium), Royal Belgian Institute for Space Aeronomy (BISA, Belgium), Royal Observatory  
145 of Belgium (ROB, Belgium), Von Karman Institute (VKI, Belgium), DH Consultancy (DHC,  
146 Belgium), Space Applications Services (SAS, Belgium), and British Antarctic Survey (BAS,  
147 United Kingdom).

148  
149 The VSWMC-P2 system is an updated design and fresh implementation of the earlier  
150 prototype VSWMC-P1 system and contains full-scale SWE models and model couplings that  
151 are ready for operational use and also some demo models enabling tests with models  
152 installed in remote locations (Brussels, Paris and Cambridge). The models and model  
153 couplings that are ready for operational use have been separated in a limited operational  
154 system that has passed the acceptance tests on 04/03/2019. The system went operational on  
155 28 May 2019 as part of the ESA SSA SWE Portal.

156  
157 In Section 2 we provide a brief general description of the scope of the project and its  
158 objectives. In Section 3 we provide an overview of the design of the fully deployed VSWMC  
159 system and in Section 4 we focus on the release of the system, with two components, viz. a  
160 test/development system and a limited operational system with the tested, stable models  
161 and model couplings integrated in the SSA Space Weather Portal. Section 4 of the present  
162 paper is dedicated to the functionality of the newly released system. We conclude with a  
163 summary of the major achievements and ideas/recommendations for future enhancements.  
164

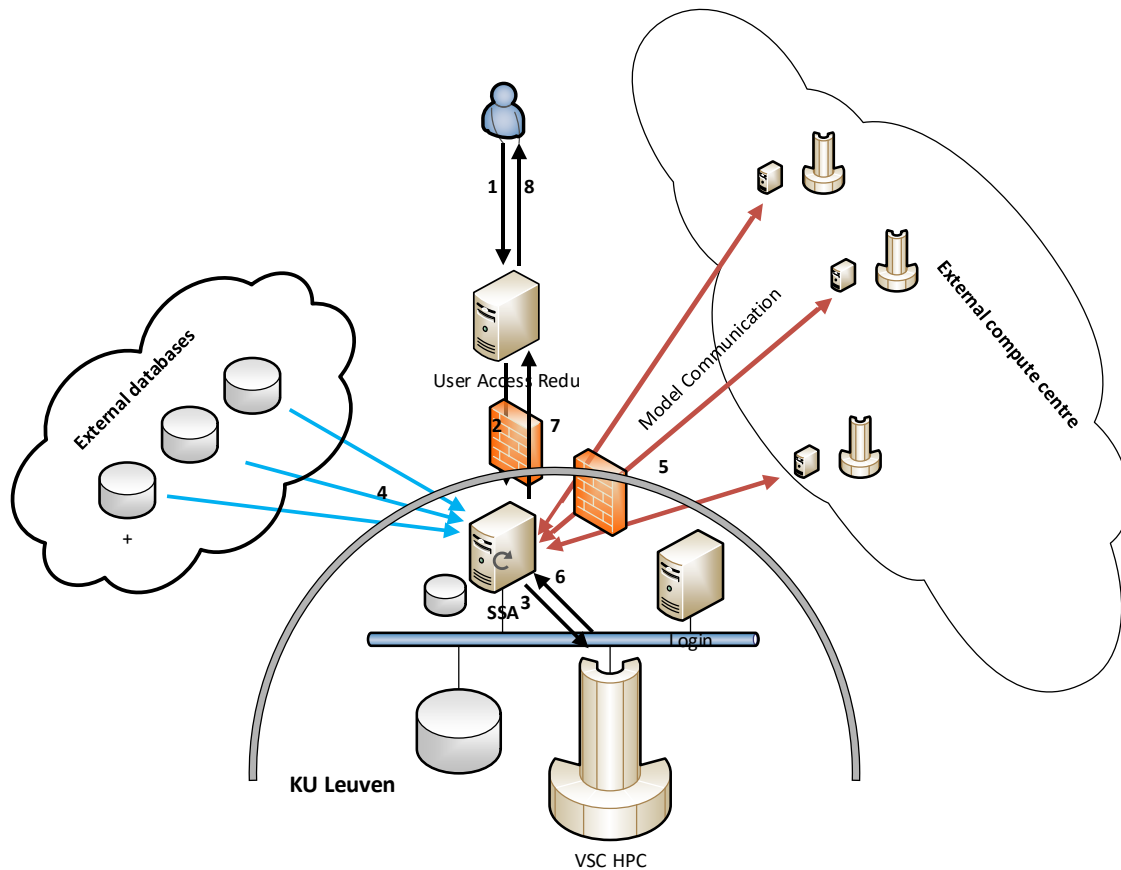
## 165 **2 GENERAL DESCRIPTION AND OBJECTIVE(S)**

### 166 **2.1 Background**

167 The Virtual Space Weather Modelling System (GEN/mod) is a service in the General Data  
168 Services (GEN) domain of the SSA SWE services [ESA SSA Team, 2011]. See also the the ESA  
169 website on SSA Space Weather services: <http://swe.ssa.esa.int/web/guest/user-domains>.

170  
171 The continued development of the VSWMC was intended to be fully in-line with the  
172 federated approach (see [Fig. 1](#)) of the SSA programme Space Weather Element (SWE) in its  
173 current Period 3. The VSWMC system is installed on a virtual server within the firewall of  
174 the KU Leuven and makes use of the data storage and High Performance Computing facilities  
175 of the Vlaams Supercomputer Centrum (VSC, <https://www.vscentrum.be/>) at the KU  
176 Leuven. The users login via the Single Sign On system which requires a ‘hand-shaking’  
177 procedure with a server at the ESA centre in Redu. Some of the integrated models are  
178 installed on the Tier 2 cluster in Leuven. Other models, however, are integrated remotely,  
179 i.e. they are installed on the local server or cluster of the modeller involved and they use the  
180 local CPU time. Nevertheless, these models controlled via the VSWMC system in Leuven.  
181 Examples are XTRAPOL that is running in Paris and BAS-RBM, running in Cambridge. The  
182 same applies to external databases that serve as input for running some of the models. For  
183 instance, solar surface magnetograms are downloaded from the Gong database  
184 (<https://gong.nso.edu/data/magmap>) and CME input parameters from the Space Weather

185 Database Of Notifications, Knowledge, Information (DONKI,  
 186 <https://kauai.ccmc.gsfc.nasa.gov/DONKI>) server at CCMC.  
 187  
 188



189 **Figure 1:** basic set-up of the federated VSWMC-P2 service with geographically distributed system  
 190 elements.  
 191

192 **2.2 Long term objective: future more advanced VSWMC**

193 The VSWMC is being developed in different phases. The present paper reports on the status  
 194 after the second phase. The future final VSWMC shall perform, as a minimum, the following  
 195 functions:

- 196 • Provide a repository for accessing space weather models
- 197 • Allow the user to interactively couple SWE models
- 198 • Allow for the execution of coupled model simulations, providing a robust framework
- 199 supporting end-to-end space weather simulations
- 200 • Ability to ingest additional or new SWE data sets/data products from remote data
- 201 providers in order to run the included models
- 202 • Provide an infrastructure for installing geographically distributed system elements as
- 203 federated elements within the SSA SWE network

- 204 • Perform verification of installed models
- 205 • Provide model output visualisations capabilities
- 206 • Provide capability to validate and compare model outputs
- 207 • Provide an interface for forecasters and other users to perform complex simulations.
- 208

### 209 **2.3 Potential user groups/users**

210 Most of the “users” or “customers”, i.e. the people that will interact with the VSWMC, can be  
211 associated with a specific space weather science and/or service domain. The Expert Service  
212 Centre on Heliospheric Weather and its Expert Groups are an obvious example of potential  
213 users of the VSWMC. It is equally evident that the Expert Groups of the other four Expert  
214 Service Centres will also benefit from the use of the VSWMC as it contains, or will contain in  
215 the near future, solar models e.g. for solar flares and CME onset (Solar-ESC), ionospheric  
216 models (Ionospheric Weather-ESC), Solar Energetic Particles models (Space Radiation-  
217 ESC) and Earth magnetosphere and geomagnetic effects models (Geomagnetic-ESC).  
218

219 In the design of the VSWMC, the ‘customers’ of foremost importance were the model  
220 developers, with ESA using model predictions, and with scientists, industrial users and the  
221 general public as additional users. These users and their potential requirements of the  
222 system have first been described in detail. Upon translating these user requirements to  
223 system requirements, a further distinction between different users was made, since this  
224 proved necessary for the implementation of the prototype system. The approach followed  
225 was to consider four categories of users: *content providers (modellers)*, *simulators (running*  
226 *models)*, *end users (using the output of model runs)*, and *VSWMC personnel (admin and*  
227 *support)*.

### 228 **2.4 Short term objective: VSWMC Part 2**

229 The new developments for Part 2 have been focused on the VSWMC prototype and the  
230 interaction with the SSA SWE system, the modification of model wrappers (so-called MCIs,  
231 model coupling interfaces) to exchange only relevant/required information, the interfacing  
232 of new models on the system, and the development of new model couplings including a first  
233 demonstration of an end-to-end (Sun-Earth) simulation capability. It also paid a lot of  
234 attention to the development of the Run-Time Interface (RTI, allowing the user to easily  
235 change simulation/model parameters before the simulation starts) in order to be able to cope  
236 with high communication loads, and the development and wider use of the coupling toolkit  
237 and the front-end. In particular, the Graphical User Interface (GUI) which has been designed  
238 to be accessible via the SWE Portal. Last but not least, this Part 2 project also assured the  
239 availability of more data on the system (for model input and for valorisation of the results)  
240 and the development of visualisation tools.

241

### 242 **2.5 Outcome**

243 The project work flow contained three distinct parts focussing on the design, the  
244 development and the demonstration of its functionality, respectively. The main outcomes of  
245 the project are: 1) an updated architectural design of the full VSWMC system and the

246 detailed design of the system based on an updated requirements analysis; 2) the new release  
247 of the VSWMC, i.e. an updated core system, new added models, additional data provision  
248 nodes and a novel graphical user interface; and 3) a demonstration of the model federate  
249 outputs in visualisation federates and validations in order to showcase the functionality of  
250 the system to perform verification and validation of models.

251 These outcomes are described in more detail below. The Scientific Advisory Team (SAT) of  
252 this activity consisted of A. Aylward, S. Bruinsma, P. Janhunen, T. Amari, D. Jackson, S.  
253 Bourdarie, B. Sanahuja, P.-L. Blelly, and R. Vainio. The SAT members were consulted via  
254 emails and during two so-called round-table meetings. During the first round table meeting  
255 with the Scientific Advisory Team, the planning of the VSWMC project and the Customer  
256 Requirements Document and System Requirements Document have been discussed with the  
257 SAT members as well as the Asset Review focussing on the missing assets. The 2<sup>nd</sup> round  
258 table meeting focused on the selection of the models to be included, the required data  
259 provision, the desired model couplings and visualizations, related challenges, as well as a  
260 first reflection on the verification and validation problems and how to handle them properly.

261  
262

### 263 **3 DESIGN OF THE FULL VSWMC SYSTEM**

#### 264 **3.1 Assets Review and Customer Requirements**

265 The VSWMC-P2 team's first task consisted of reviewing the existing space weather models  
266 and data-related assets across Europe including assets produced within projects of the 7<sup>th</sup>  
267 Framework Programme funded by the European Commission from 2007 until 2013, assets  
268 from the SSA SWE Assets Database, the assets already identified during the VSWMC-P1  
269 project and additional assets suggested by the Science Advisory Team during the first Round  
270 Table meeting. The review process led to an Assets Review Report and assessed the  
271 suitability of each asset for its exploitation in the VSWMC, especially with regards to real-  
272 time space weather forecasting. Moreover, based on the review a gap analysis was presented  
273 to indicate areas of lacking maturity in present European modelling capabilities.

274  
275 The VSWMC-P2 team and the SAT also reflected upon the Customer Requirements and the  
276 relations of the VSWMC customer requirements to the customer requirements of the whole  
277 SSA SWE service system. The set of domains can be divided in two major groups, viz. the  
278 domains corresponding to the physical components of the space environment and the space  
279 weather service domains, representing the ESA Space Situational Awareness classification.  
280 The origin and the relevance of the requirements has been illustrated by a number of 'user  
281 stories', presenting the actual needs of e.g. a general end user (amateur astronomer, public),  
282 a space instrument designer, or an experienced space weather scientist.

283



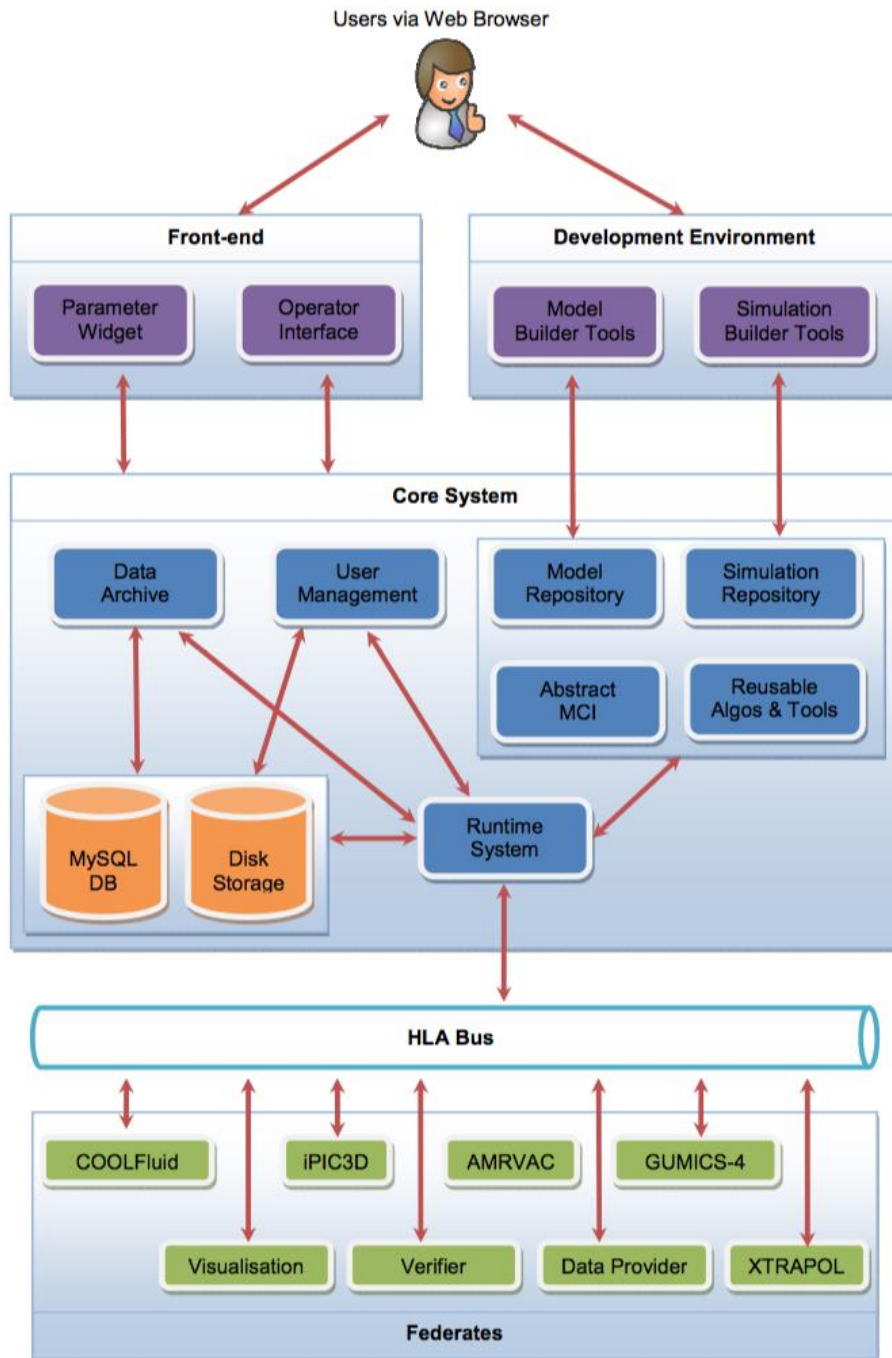


Figure 2: VSWMC-P2 system requirements overview.

284  
285

286

### 287 3.2 System requirements

288 The VSWMC system requirements address the following audiences: system developers and  
 289 operators, model implementers, and end users. One of the most challenging system  
 290 requirements concerned the desire to develop an infrastructure for installing *geographically*

291 *distributed system elements* as federated elements within the SSA SWE network. To achieve  
292 this challenge, the VSWMC is built on ‘high-level architecture’ (HLA). This terminology  
293 refers to a general purpose software architecture that has been developed to enable  
294 distributed computer simulation systems, i.e. with different components of the simulation  
295 running on different (remote) computers with different operating systems. As a matter of  
296 fact, within the HLA framework different computer simulations, or different components of  
297 a large simulation, can interact (i.e. interchange data, synchronize actions) regardless of the  
298 computing platforms on which they run and regardless of the programming language they  
299 are developed in. The interaction between the different components of the simulation is  
300 managed by a Run-Time Infrastructure (RTI). In other words, HLA provides a general  
301 framework and standard (IEEE Standard 1516-2000) facilitating interoperability (and  
302 reusability) of distributed computer simulation components. It is currently used in  
303 applications in a number of different domains such as, defence, air traffic management, off-  
304 shore, railway and car industry, and manufacturing.

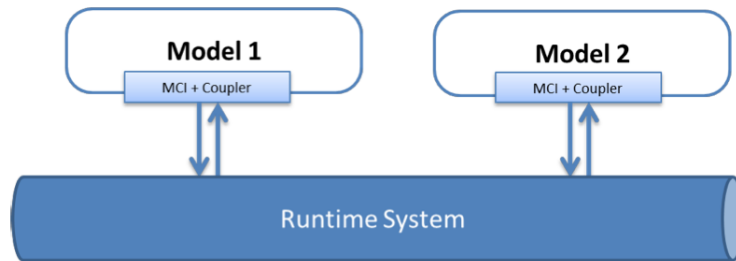
305  
306  
307 The other systems requirements are summarized in [Figure 2](#). The users login via the web  
308 portal (in the SSA SWE system). The Core system contains 4 service components, viz. the  
309 model and simulation repositories, the Model Coupling Interfaces (MCI) and a collection of  
310 reusable algorithms and tools. The model developers have to write a model-specific MCI  
311 implementation. The computational models/solvers and data streams are treated uniformly  
312 through the same Abstract MCI. The Core system also contains a data archive and a user  
313 management component. Only the runtime system interacts with HLA bus to coordinate  
314 simulations. Note that model visualizations are implemented as ‘federates’ (HLA  
315 terminology), i.e. as any other model, taking synthetic data form simulations and producing  
316 plots and/or movies.

### 319 **3.3 Architectural and detailed design**

320 A system Interface Control Document (ICD) has been developed that provides third party  
321 model integrators and infrastructure providers all necessary information to be able to  
322 integrate and run new models in the VSWMC system. This document covers the interaction  
323 between system, Model Coupling Interfaces and model and describes the MCI functions, the  
324 MCI communication to the core system and the Coupling Toolkit functionality available to  
325 the MCI, as well as access methods and environmental requirements.

326  
327 The Run-time system (RTS) prepares the models for execution and manages the data  
328 exchange between the models, *over the internet* in case the models are installed in different  
329 locations (see Figure 3). The run-time system is capable of executing parameterized  
330 simulation runs. As a simulation is interpreted, different models are retrieved from the  
331 Model Repository (cf. Section 3.2 and Figure 2).

332

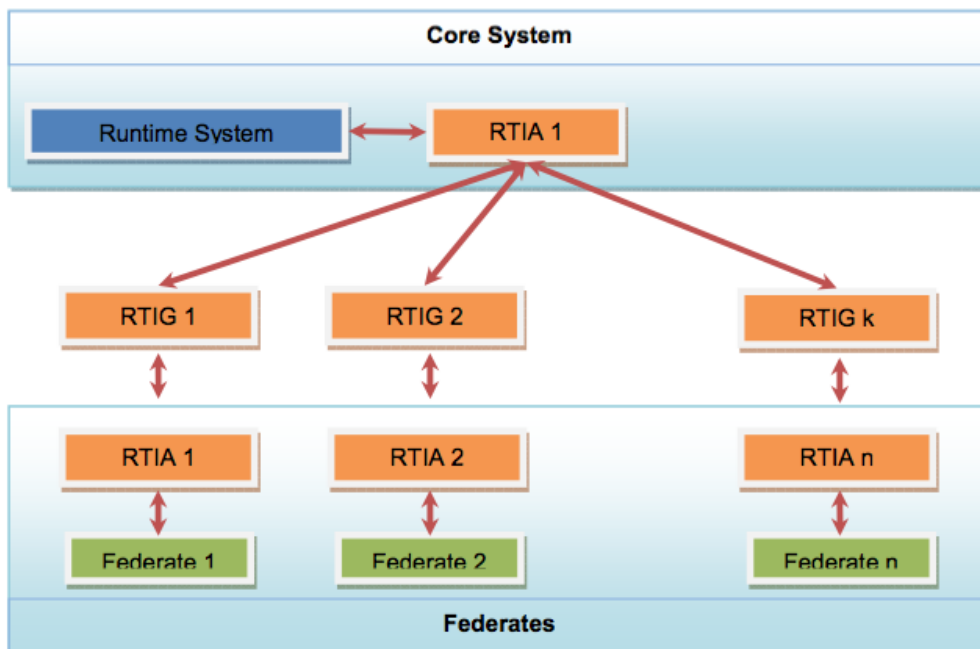


333  
334  
335

**Figure 3:** Illustration of the Run-time system taking models from the repository and linking them to each other via Model Coupling Interfaces.

336  
337  
338  
339  
340  
341  
342  
343  
344  
345  
346  
347  
348  
349  
350  
351

The architectural design of the complete VSWMC system has been updated. During the VSWMC-Part 1 project, a prototype of the VSWMC system had been developed. This consisted of a simulation framework using at its core CERTI, an open source implementation of the High Level Architecture (HLA) middleware. The latter allows for connecting various models (through data exchange) which can run remotely distributed and concurrently, potentially achieving a good performance in complex simulations. The coupling is not intrusive, in the sense that each model is treated as a black-box, therefore unmodified, and encapsulated in a separate component through a Model Coupling Interface (MCI). At present, custom scripts must be provided by the modellers to integrate and run their models within VSWMC. Before exchanging the data, data conversions or transformations necessary for achieving the coupling are taken care by the Coupling Tools Kit (CTK). The latter has been implemented as a standalone flexible infrastructure where each new feature is treated as a configurable and dynamic plug-in. A GUI is also available for simplifying the usage of the VSWMC system by end-users.



352  
353  
354

**Figure 4:** RTI Gateways (RTIGs) manage the simulations and transfers messages between federates. The VSWMC-P2 system supports multiple RTIGs to tackle high communication loads.

355 When a user wants to run a simulation, he/she has to provide inputs as required by the  
356 simulation. An input file will be created by the front-end based on a template, by replacing  
357 template variables with user provided (via an input widget) values. The user can see the  
358 resulting file (together with the simulation outputs) but does have the possibility to change  
359 the file as we want to prevent invalid input files to be used. Only the operator can  
360 generate/modify the templates used for the configuration files.  
361  
362

## 363 **4 RELEASE OF THE VSWMC**

### 364 **4.1 Development of the VSWMC core system**

365 Priority has been given to the interfaces between the core-system to models federates, to the  
366 data provision federate, and the front-end component. The underlying processing has been  
367 implemented to make all the defined interfaces operational.  
368

369 The Run-time System was enhanced with, amongst others, a Parallel Real-time  
370 Infrastructure Gateway (RTIG, illustrated in Figure 4) to share the communication loads,  
371 extensible simulation-specific configuration through the use of Python scripts, real-time  
372 data connectivity to connected clients (e.g. live streaming of log files), and connectivity to  
373 VSWMC nodes installed both on-premise and off-premise (the VSWMC system is spread out  
374 on different compute cluster nodes or platforms).  
375

376 The software architecture is made up of the following parts:

- 377 • A front end for regular users to interact with the VSWMC to run simulations.
  - 378 • Couplers software which deals with timing of model calls and data exchange.
  - 379 • A library of coupling tools for data transformation from one model to another.
  - 380 • A model coupling interface for the models themselves and datasets for model input.
- 381  
382

383 The VSWMC system treats each model as a black-box. Hence, to integrate and run it within  
384 the VSWMC system (which is done by encapsulating the model in a separate component  
385 through a Model Coupling Interface (MCI)), the model developer has to provide all the  
386 information (metadata) that describes properties of the model necessary for enabling its  
387 integration and operation through the VSWMC system.  
388  
389

### 390 **4.2 Interfacing of additional space weather models**

391 Extra physics-based as well as empirical and data-driven codes have been added to the  
392 VSWMC as the prototype system only contained a few demonstration models to show the  
393 capabilities of the system. The VSWMC system now contains the following models (some are  
394 still not fully operational as some modellers only provided a limited demo model):

- 395 • **AMRVAC Solar Wind** (demo): Steady 2.5D (axisymmetric) solar wind (quiet Sun)  
396 to 1 AU [Xia et al., 2018; Hosteaux et al., 2018, 2019];

- 397 • **AMRVAC CME** (demo): 2.5D (axisymmetric) flux rope CME superposed on the  
398 AMRVAC Solar Wind as an initial condition and propagating to 1 AU [Xia et al., 2018;  
399 Hosteaux et al., 2019];
- 400 • **COOLFluid Steady** (demo): calculates the position and shape of the bow shock at  
401 Earth for specified steady solar wind conditions (3D) [Lani et al., 2013; Yalim &  
402 Poedts, 2013];
- 403 • **CTIP** (demo): Coupled Thermosphere Ionosphere Plasma sphere model, a global,  
404 three-dimensional, time-dependent, non-linear code that is a union of three physical  
405 components (a thermosphere code, a mid- and high-latitude ionosphere convection  
406 model, and a plasma sphere and low latitude ionosphere) [Millard et al., 1996; Fuller-  
407 Rowell & Rees, 1980];
- 408 • **EUHFORIA**: 3D steady heliospheric wind with superposed (Cone) CME propagation  
409 [Pomoell & Poedts, 2018; Scolini et al., 2018];
- 410 • **Dst index**: empirical model to determine the Dst index from solar wind data at L1  
411 [provided by C. Scolini, based on O'Brien & McPherron, 2000];
- 412 • **Kp index**: empirical model to determine the Kp index from solar wind data at L1  
413 [provided by C. Scolini, based on Newell et al., 2008];
- 414 • **Plasma pause stand-off distance**: empirical model using solar wind data at L1  
415 [provided by C. Scolini, based on Taktakishvili et al., 2008];
- 416 • **BAS-RBM**: 3 dimensional, time-dependent diffusion model for phase-space density  
417 based on solution of the Fokker-Planck equation that produces a time-series of the  
418 flux or phase-space density on the 3-d grid [Glauert et al., 2014];  
419 [Note: this model has been taken out of operation as BAS left the project team.]
- 420 • **GUMICS-4**: a global magnetosphere–ionosphere coupling simulation based on  
421 global MHD magnetosphere and an electrostatic ionosphere [Janhunen et al., 2012;  
422 Lakka et al., 2019];
- 423 • **COOLFluid unsteady**: 3D time-accurate Earth magnetosphere model [Lani et al.,  
424 2013; Yalim & Poedts, 2013];
- 425 • **ODI**: takes data from the Open Data Interface (ODI), a database system for retrieving,  
426 processing and storing space environment (and other) data and metadata in a MySQL  
427 (MariaDB, one of the most popular open source relational databases) database  
428 [<https://spitfire.estec.esa.int/trac/ODI/wiki/OdiManual>];
- 429 • **XTRAPOL** (demo): extrapolation of coronal magnetic field in an active region  
430 [Amari et al., 2006].

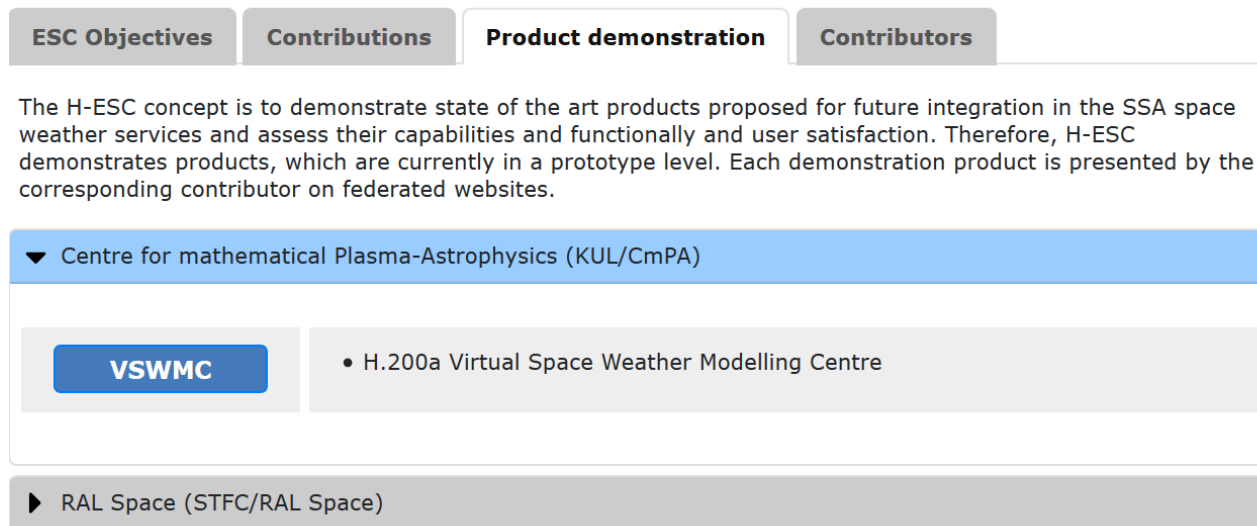
431  
432 An Interface Control Document (ICD) has been provided for each VSWMC model showing  
433 e.g. its overall functions, outputs, inputs, hardware requirements, the amount of CPU hours  
434 required, and including the model structure where appropriate, its Technology readiness  
435 level (TRL) and a reference. A set of new Model Coupling Interfaces has been developed to  
436 interface the VSWMC models. More information on each of the operational models is given  
437 below in Section 4.3.  
438

### 439 **4.3 Operational models**

440 The VSWMC went operational in May 2019 and is available to everybody via the SSA Space  
441 Weather portal. Of course, users first need to provide credentials but these can be obtained

442 after simple request. For the time being, the VSWMC is reachable via the H-ESC  
443 (Heliospheric-Expert Service Centre) webpage where it is shown as “Product demonstration”  
444 under “Centre for mathematical Plasma-Astrophysics (KUL/CmPA)”, see Figure 5:

## Heliospheric Weather Expert Service Centre (H-ESC)



445 **Figure 5:** Screen shot of the H-ESC webpage with the Link “VSWMC” on the ‘Product  
446 demonstration’ tab that gives access to the login page of the VSWMC.  
447

448 It will be put more forward in the future. Clicking on the “VSWMC” button brings the user  
449 to the login page: <http://swe.ssa.esa.int/web/guest/kul-cmpa-federated>.

450 As mentioned above, this operational system only contains the models that are full-fledged,  
451 verified and validates via the standard procedures. These are the following models.

452

### 453 **4.3.1 EUHFORIA-Corona**

#### 454 **Model description**

455 The EUHFORIA (European Heliospheric FORecasting Information Asset) model aims to  
456 provide a full Sun-to-Earth modelling chain combining efficient data-driven, semi-  
457 empirical, forward approaches with physics-based models wherever appropriate. It consists  
458 of two parts, viz. a coronal module and a heliospheric solar wind module that enables  
459 superimposed CME evolution. The modules can be run together or each module can be run  
460 separately if wanted. This section describes the EUHFORIA Corona module interface.

461 The aim of the coronal module is to provide the required MHD input quantities at 21.5 Rs  
462 for the heliospheric solar wind module. The coronal module in EUHFORIA is data-driven  
463 and combines a PFSS magnetic field extrapolation from GONG or ADAPT magnetograms (1  
464 – 2.5 Rs) with the semi-empirical Wand-Sheely-Arge (WSA) model and the Schatten current  
465 sheet (SCS) model to extend the velocity and magnetic field from 2.5 Rs to 21.5 Rs. This is  
466 done in combination with other semi-empirical formulas so that also the density and the  
467 temperature is given at 21.5 Rs

## 468 **Model access and run information**

469 In the VSWMC framework, EUHFORIA Corona is supposed to be installed and run on one  
470 of the KU Leuven HPC servers, access to which is provided via ssh.

## 471 **Model input**

472 As an input EUHFORIA Corona takes either standard GONG (as stored in URL  
473 <http://gong.nso.edu/data/magmap/QR/>) or GONG ADAPT Magnetogram Synoptic Maps  
474 (as stored in <ftp://gong2.nso.edu/adapt/maps/gong/>) in the FITS file format. Files  
475 compressed with gzip also supported. The magnetogram provider (GONG or GONG\_ADAPT)  
476 is defined in configuration file with the keyword `provider`.

477 Magnetogram source is defined in the configuration file with the keyword `source`. Four  
478 source types are supported:

- 479 **1.** If an URL is provided, the file is downloaded using that URL.
- 480 **2.** If it is a locally stored magnetogram file, the file is used.
- 481 **3.** If a date & time string (e.g. 2012-06-12T12:23:00) is provided, the file corresponding  
482 to the date is downloaded using the URL of magnetogram provider defined in the  
483 provider field.
- 484 **4.** If keyword "latest" is provided, the most recently available magnetogram is  
485 downloaded using the URL of magnetogram provider defined in the provider field.

## 486 **Model output**

487 The output of the EUHFORIA Corona model is the solar wind boundary data file that  
488 provides MHD input quantities at 21.5 Rs for the EUHFORIA Heliosphere solar wind  
489 module.

## 490 **Related paper**

492 J. Pomoell and S. Poedts: "EUHFORIA: EUropean Heliospheric FORecasting Information  
493 Asset", J. of Space Weather and Space Climate, 8, A35 (2018). DOI:  
494 <https://doi.org/10.1051/swsc/2018020>

495  
496

## 497 **4.3.2 EUHFORIA-Heliosphere**

### 498 **Model description**

499 The heliosphere module of EUHFORIA provides the solar wind from 21.5 Rs to 2 AU (or  
500 further if necessary). Input at 21.5Rs is provided by a coronal module, for example,  
501 EUHFORIA-Corona. It initially extends the (purely radial) velocity and magnetic field to 2  
502 AU and subsequently relaxes this initial MHD solution by applying a rotating inner boundary  
503 to create the solar background wind in a relaxed state. This yields a steady solar wind from  
504 21.5 Rs to 2 AU in the co-rotating frame, as the inner boundary condition is not updated, but  
505 merely rotated. The coordinate system of the model is HEEQ.

506 Apart from providing the background solar wind, the EUHFORIA-heliosphere model is also  
 507 able to launch CME models superimposed on the background solar wind. Therefore, it can  
 508 simulate CME evolution up to 2 AU (and beyond, if required). It currently has the classic  
 509 cone CME model fully supported and a novel Gibson-Low flux-rope CME model is being  
 510 under development. In contrast with the classic cone model, the Gibson-Low flux-rope  
 511 model not only enables to model the CME shock evolution but also the internal magnetic  
 512 structure of the IP magnetic cloud following the shock. The magnetic field of the CME is not  
 513 modelled with the cone model. The Gibson-Low model was added into EUHFORIA recently  
 514 and is not yet capable of predicting the flux rope parameters for efficient forecasting.  
 515 However, in the future efforts will be made towards this goal and the VSWMC will be a great  
 516 way to test the prediction capabilities of this flux-rope model.

### 517 **Model access and run information**

518 In the VSWMC framework, EUHFORIA Heliosphere is supposed to be installed and run in  
 519 the KU Leuven HPC, access to which is provided via ssh.

### 520 **Model input**

521 As an input EUHFORIA Heliosphere accepts two files: file, containing solar wind boundary  
 522 data, this data file is mandatory, and file, containing a list of CMEs relevant for the particular  
 523 simulation run.

- 524 • **Solar wind boundary data** file. This file is mandatory and normally it is provided  
 525 as the EUHFORIA Corona v.1.0 model output.
- 526 • **CME list** file. This data is optional, the file is also in ASCII text format and have to  
 527 be created by the user manually (or with the help of VSWMC framework) in  
 528 accordance with CME model template. Several CME models are supported by  
 529 EUHFORIA Heliosphere v.1.0, and hence there are several templates that describe  
 530 somewhat different CME parameters but in current VSWMC phase we support only  
 531 Cone CME model.

### 532 **Model output**

533 As an output EUHFORIA Heliosphere generates physical parameters of solar wind from 21.5  
 534 Rs to 2 AU (or further if necessary), see Model Description section. The parameters are the  
 535 following:

Output solar wind parameter	Data unit	Data type
Date	YYYY-MM-DDThh:mm:ss (ISO8601 date and time format)	string
Grid point radial coordinate r	AU (Astronomical Unit)	float
Grid point colatitude clt	rad (radian)	float
Grid point longitude lon	rad (radian)	float
Number density n	1/cm <sup>3</sup> (particles per cubic centimeter)	float
Pressure P	Pa (Pascal)	float



Radial component of velocity vr	km/s (kilometers per second)	float
Colatitude component of velocity vclt	km/s (kilometers per second)	float
Longitude component of velocity vlon	km/s (kilometers per second)	float
Radial component of magnetic field Br	nT (nano Tesla)	float
Colatitude component of magnetic field Bclt	nT (nano Tesla)	float
Longitude component of magnetic field Blon	nT (nano Tesla)	float

536

537 **Related paper**

538 J. Pomoell and S. Poedts: "EUHFORIA: EUropean Heliospheric FORecasting Information  
539 Asset", *J. of Space Weather and Space Climate*, 8, A35 (2018). DOI:  
540 <https://doi.org/10.1051/swsc/2018020>

541

542

543 **4.3.3 GUMICS-4**

544 **Model description**

545 The global magnetosphere-ionosphere coupling model GUMICS-4 solves ideal MHD  
546 equations in the magnetosphere and couples them to an electrostatic ionosphere. The inner  
547 boundary of the MHD domain is at 3.7 Earth radii. Between the ionosphere and 3.7 Earth  
548 radii, quantities involved in the ionosphere-magnetosphere coupling loop (potential,  
549 precipitation, field-aligned currents) are mapped along unperturbed magnetic field lines.  
550 The MHD part uses an unstructured finite volume octogrid which is automatically refined  
551 and coarsened during the run using also refinement priorities hand-coded for the  
552 magnetosphere. The MHD solver is the Roe solver. In cases where one or more of the  
553 intermediate states returned by the Roe solver are not physical (negative density or  
554 pressure), the robust HLL solver is used instead. Analytic splitting of the magnetic field in  
555 dipole field and perturbation field is used. The MHD code is time accurate and uses temporal  
556 subcycling to speed up computation.

557 The ionospheric model consists of a 2-D elliptic solver for the electric potential. The source  
558 term is proportional to the field-aligned current obtained from the MHD variables and  
559 mapped down to ionospheric plane. The coefficients of the elliptic equation contain the  
560 height-integrated Pedersen and Hall conductivities. The ionospheric electron density is  
561 initially computed in a 3-D grid using production and loss terms. The conductivities needed  
562 by the elliptic solver are obtained by explicit height integration of the 3-D conductivities. The  
563 electron density takes contribution from modelled solar UV radiation, from a constant  
564 background profile and electron precipitation which is modelled from the MHD variables  
565 which map to the point.

566 **Model access and run information**

567 In the VSWMC framework, GUMICS-4 is installed and run on the same virtual server where  
568 the framework itself runs.

569

570 **Model input**

571 The main input for GUMICS-4 is the solar wind time series at the Lagrange L1 point or other  
572 upstream point. The input can be artificial or obtained from a satellite such as ACE or SOHO,  
573 for example via ODI. The solar wind data are read from a separate text file.

574 The parameters required for GUMICS-4 are the following: particle density, temperature,  
575 velocity and magnetic field vectors in GSE coordinate system. The data values are in SI data  
576 units. The file contains the following parameters:

577

<b>Input solar wind parameter</b>	<b>Data unit</b>	<b>Data type</b>
Time	seconds	integer
Number density	m <sup>-3</sup> (particles per cubic meter)	float
Temperature	K (Kelvin)	float
Velocity component V_GSE_x	m*s <sup>-1</sup> (meters per second)	float
Velocity component V_GSE_y	m*s <sup>-1</sup> (meters per second)	float
Velocity component V_GSE_z	m*s <sup>-1</sup> (meters per second)	float
Magnetic field component B_GSE_x	T (Tesla)	float
Magnetic field component B_GSE_y	T (Tesla)	float
Magnetic field component B_GSE_z	T (Tesla)	float

578

579 **Model output**

580 GUMICS-4 saves the 3-D MHD variables in its unstructured grid in a custom binary file "HC"  
581 format ("Hierarchical Cartesian" format) which is efficient to store and fast to read. The  
582 ionospheric quantities are similarly stored in a "TRI" file (for TRIangular finite element grid  
583 data).

584 The full list of output parameters contains more than 50 entries. The list of main physical  
585 parameters for each output time stamp is the following :

586

<b>Main output solar wind parameter</b>	<b>Data unit</b>	<b>Data type</b>
Time stamp of the output file	second	integer
x: X-coordinate	m (meter)	float
y: Y-coordinate	m (meter)	float
z: Z-coordinate	m (meter)	float
rho: Mass density	kg/m <sup>3</sup> (kilogram per cubic meter)	float
rhovx: X-component of the momentum flux	kg/(m <sup>2</sup> *s)	float
rhovy: Y-component of the momentum flux	kg/(m <sup>2</sup> *s)	float
rhovz: Z-component of the momentum flux	kg/(m <sup>2</sup> *s)	float
U: Total energy density, thermal + kinetic + magnetic	J/m <sup>3</sup>	float
Bx: X-component of the total magnetic field	T (Tesla)	float
By: Y-component of the total magnetic field	T (Tesla)	float
Bz: Z-component of the total magnetic field	T (Tesla)	float

587

588 **Related paper**

589 Janhunen, P.; Palmroth, M.; Laitinen, T.; Honkonen, I.; Juusola, L.; Facskó, G.; Pulkkinen,  
590 T. I., “*The GUMICS-4 global MHD magnetosphere-ionosphere coupling simulation*”,  
591 Journal of Atmospheric and Solar-Terrestrial Physics, Volume **80**, p. 48-59 (2012).

592

593 **4.3.4 BAS-RBM**

594 **Model description**

595 The BAS Radiation Belt Model (BAS-RBM) solves a Fokker-Planck equation for the time-  
596 dependent, drift-averaged, high energy ( $E > \sim 100$  keV) electron flux in the Earth’s radiation  
597 belts. A detailed description of the model is given in *Glauert et al.*, [2014a, b]. The model  
598 includes the effects of radial transport, wave-particle interactions and losses to the  
599 atmosphere and magnetopause. Radial transport is modelled as radial diffusion using the  
600 coefficients of *Ozeke et al.* [2014]. Wave-particle interactions due to upper and lower band  
601 chorus [*Horne et al.*, 2013], plasmaspheric hiss and lightning-generated whistlers [*Glauert*  
602 *et al.*, 2014a] and electro-magnetic ion cyclotron waves [*Kersten et al.*, 2014] are included in

603 the model. Losses to the atmosphere follow *Abel and Thorne* [1998] and losses to the  
604 magnetopause are modelled as described in *Glauert et al.* [2014b].

605 The outer radial ( $L^*$ ) boundary condition is determined from GOES 15 data. The inner radial  
606 boundary and the low energy boundary are set using statistical models derived from CRRES  
607 data, see *Glauert et al.* [2014b]. The drift-averaged differential flux is calculated as a function  
608 of pitch-angle ( $\alpha$ ), energy ( $E$ ),  $L^*$  and time. Pitch-angles lie in the range  $0^\circ \leq \alpha \leq 90^\circ$ .  $L^*$  is  
609 calculated using the Olson-Pfizer quiet time model and lies in the range  $2 \leq L^* \leq 6.5$ . At  $L^*$   
610 = 6.5,  $103.2 \text{ keV} \leq E \leq 30 \text{ MeV}$  and the energy range increases with increasing  $L^*$ .

611 The model requires the Kp index, electron and proton fluxes and position data from GOES  
612 15 (to provide the outer boundary condition) and the magnetopause location for the period  
613 of the simulation. The start time can be any time between 00:00 on 1-1-2011 and the present.  
614 Simulations are limited to 1 week.

615

## 616 **References**

- 617 • Glauert, S. A., R. B. Horne, and N. P. Meredith (2014a), Three-dimensional electron  
618 radiation belt simulations using the BAS Radiation Belt Model with new diffusion  
619 models for chorus, plasmaspheric hiss, and lightning-generated whistlers, *J.*  
620 *Geophys. Res. Space Physics*, 119, 268–289, doi:10.1002/2013JA019281.
- 621 • Glauert, S. A., R. B. Horne, and N. P. Meredith (2014b), Simulating the Earth's  
622 radiation belts: Internal acceleration and continuous losses to the magnetopause, *J.*  
623 *Geophys. Res. Space Physics*, 119, 7444–7463, doi:10.1002/2014JA020092.
- 624 • Horne, R. B., T. Kersten, S. A. Glauert, N. P. Meredith, D. Boscher, A. Sicard-Piet, R.  
625 M. Thorne, and W. Li (2013), A new diffusion matrix for whistler mode chorus waves,  
626 *J. Geophys. Res. Space Physics*, 118, 6302–6318, doi: 10.1002/jgra.50594.
- 627 • Kersten, T., R. B. Horne, S. A. Glauert, N. P. Meredith, B. J. Fraser, and R. S.  
628 Grew (2014), Electron losses from the radiation belts caused by EMIC waves, *J.*  
629 *Geophys. Res. Space Physics*, 119, 8820–8837, doi:10.1002/2014JA020366.
- 630 • Ozeke, L. G., I. R. Mann, K. R. Murphy, I. Jonathan Rae, and D. K. Milling (2014),  
631 Analytic expressions for ULF wave radiation belt radial diffusion coefficients, *J.*  
632 *Geophys. Res. Space Physics*, 119, 1587–1605, doi:10.1002/2013JA019204.

633

## 634 **Model access and run information**

635 For the VSWMC the BAS-RBM is accessed by placing a run request on an ftp server  
636 ([ftp://vswmcftp@ftp.nerc-bas.ac.uk/vswmc\\_data/](ftp://vswmcftp@ftp.nerc-bas.ac.uk/vswmc_data/)) at the British Antarctic Survey. Each  
637 request has a unique id generated by the VSWMC and referred to as *run\_id* for the rest of  
638 this document. The VSWMC creates a directory called *run\_id* in [ftp://vswmcftp@ftp.nerc-](ftp://vswmcftp@ftp.nerc-bas.ac.uk/vswmc_data/)  
639 [bas.ac.uk/vswmc\\_data/](ftp://vswmcftp@ftp.nerc-bas.ac.uk/vswmc_data/) and places the following files in that directory:

640 A *run\_name*.VSWMC file which defines the run to be performed

641 A *run\_name*.KP file defining the KP sequence for the simulation

642 A *run\_name*.GOES\_COORD file with the required GOES 15 data for the run

643 A *run\_name*.MP file with the magnetopause standoff distance for the simulation

644 Here *run\_name* is an identifier supplied by the VSWMC to name this particular run. It can  
645 be the same as the *run\_id*, but does not need to be. The *run\_name* identifies all the files  
646 (both input and output) associated with a particular model run.

647 The BAS server will automatically detect when the files are placed in the directory and  
648 initiate a run, creating a log file *run\_name.log*, containing information about the progress  
649 of the run. This file can be read by the VSWMC as required to allow progress to be monitored.  
650 Only one run can be calculated at any time – if requests are received while a run is in progress  
651 then they will be queued and run in turn.

652 The output files will be placed in the same directory as the input files (i.e.  
653 [ftp://vswmcftp@ftp.nerc-bas.ac.uk/vswmc\\_data/run\\_id](ftp://vswmcftp@ftp.nerc-bas.ac.uk/vswmc_data/run_id) ). A model run will produce 3  
654 output files:

655 A *run\_name.3d* file. This is the main output from the model and contains the  
656 differential flux as a function of pitch-angle, energy,  $L^*$  and time for the simulation.

657 A *run\_name.PRE* file. This gives the precipitating electron flux at the edge of the loss  
658 cone as a function of energy,  $L^*$  and time.

659 A *run\_name.EFLUX*. This contains the differential energy flux as a function of pitch-  
660 angle, energy,  $L^*$  and time for the simulation.

661 When the run is finished these output files, together with the log file, are combined into  
662 *run\_name.tar.gz* and placed in the *run\_id* directory on the FTP site.

### 663 **Model input**

664 The BAS-RBM requires 5 input parameters and 3 input data files. The input parameters,  
665 specified in the *run\_name.VSWMC* file, are:

- 666 • The starting time of the run
- 667 • The length of the run
- 668 • The timestep for the run
- 669 • The output frequency – i.e. output the flux every *n* timesteps
- 670 • The initial condition

671

672 For the initial state of the radiation belt at the start of the calculation the user can choose  
673 one of 12 options. Each option is the steady state solution for the given  $K_p$  value, with the  
674 flux at the outer boundary ( $L^* = L_{max}$ ) set at a given percentile of the >800 keV flux  
675 distribution at GEO, derived from GOES 15 data. The  $K_p$  value for the steady state can be 1,  
676 2, 3 or 4 and the flux at the outer boundary can be the 10<sup>th</sup>, 50<sup>th</sup> or 90<sup>th</sup> percentile value. The  
677 options available for the initial condition, along with the 24 hour average, >800 keV flux at  
678 GEO for the given percentile are shown in the table below.

679

Option	$K_p$	Flux percentile	>800 keV flux at GEO ( $\text{cm}^{-2} \text{sr}^{-1} \text{s}^{-1}$ )
1	1	10	1952.7
2	1	50	17833.9

3	1	90	75068.6
4	2	10	2904.6
5	2	50	20496.2
6	2	90	78197.9
7	3	10	3676.5
8	3	50	24131.7
9	3	90	108545.2
10	4	10	2247.8
11	4	50	19293.3
12	4	90	98334.8

680

681

## 682 **Model output**

683 At the end of a successful run the model will produce three output files; *run\_name.3d*,  
684 *run\_name.PRE* and *run\_name.EFLUX*. These are all ASCII files that start with a header  
685 containing information about the run and then give a drift-averaged flux at the specified  
686 output times. The *.3d* files contain the differential flux in SI units ( $\text{m}^{-2}\text{sr}^{-1}\text{s}^{-1}\text{J}^{-1}$ ) at all the  
687 points of the pitch-angle, energy,  $L^*$  grid used in the calculation. Similarly, the *.EFLUX* files  
688 contain the differential energy flux in ( $\text{m}^{-2}\text{sr}^{-1}\text{s}^{-1}$ ). The *.PRE* files show the differential flux  
689 ( $\text{m}^{-2}\text{sr}^{-1}\text{s}^{-1}\text{J}^{-1}$ ) at the edge of the bounce loss cone.

## 690 **The computational grid**

691 The modelling domain is specified in terms of pitch-angle ( $\alpha$ ), energy ( $E$ ) and  $L^*$  coordinates.  
692 The model assumes symmetry at  $\alpha=90^\circ$ , so  $0 \leq \alpha \leq 90^\circ$ . The  $L^*$  range is  $2 \leq L^* \leq 6.5$ . The  
693 maximum energy ( $E_{max}$ ) is set at  $E_{max} = 30$  MeV at  $L^* = L_{max} = 6.5$ . The minimum energy is  
694  $E_{min} = 103.2$  keV at  $L^* = 6.5$ , corresponding to a first adiabatic invariant,  $\mu = 100$  MeV/G. The  
695 minimum and maximum energies at other  $L^*$  values are determined by following lines of  
696 constant first adiabatic invariant for points that lie in the computational grid at  $L_{max}$ . Hence,  
697 the energy at the boundaries depends on  $L^*$ , increasing as  $L^*$  decreases, so that at  $L_{min}$ ,  $E_{min}$   
698  $= 708.6$  keV and  $E_{max} = 178.2$  MeV.

699 The pitch-angle grid used in the calculation is regular, independent of energy and  $L^*$ , and  
700 covers the range  $0 \leq \alpha \leq 90^\circ$ . All grid indices run from 0 to the maximum index shown in the  
701 output file, so the pitch-angle grid is given by  $\alpha_i = i 90/N_\alpha$ ,  $i = 0, N_\alpha$ . Similarly the  $L^*$  grid is  
702 given by  $L_k = L_{min} + k (L_{max}-L_{min})/N_L$ ,  $k = 0, N_L$ .

703 The energy grid is a little more complicated as it is  $L^*$  dependent and uniform in  $\ln(\text{energy})$ .  
704 In the output files, starting at line 29, there is a table of the maximum and minimum energy  
705 values for each  $L^*$  in the grid. The energy grid at each  $L^*$  is a uniform grid in  $\ln(\text{energy})$   
706 between the maximum energy,  $E_{max}(L)$ , and the minimum energy,  $E_{min}(L)$ , with  $N_E+1$  grid  
707 points. So, if  $E_j$  is the  $j$ th grid point,

708

709

710

711

712

713

$$E_j = \exp( \ln(E_{min}) + j(\ln(E_{max}) - \ln(E_{min})) / N_E ), j = 0, N_E.$$

## 711 **The .3d file**

712 The *.3d* files contain the differential flux in SI units ( $\text{m}^{-2}\text{sr}^{-1}\text{s}^{-1}\text{J}^{-1}$ ) at the points of the  
713 computational grid. The file starts with a header that describes the setup for the run. All lines

714 up to and including line 25 have a 40 character description, followed by the appropriate  
 715 value. These are detailed in the table below.

716

Line	Contents	Format
1	Model description	String
2	Blank	
3	Maximum pitch-angle index ( $N_\alpha$ )	40 characters followed by an integer
4	Maximum energy index ( $N_E$ )	40 characters followed by an integer
5	Maximum L* index ( $N_L$ )	40 characters followed by an integer
6	Minimum energy at maximum L* (keV)	40 characters followed by a real
7	Maximum energy at maximum L*(keV)	40 characters followed by a real
8	Minimum L* value	40 characters followed by a real
9	Maximum L* value	40 characters followed by a real
10	Start time for simulation	40 characters then yyyy-mm-dd hr:mm
11	Time step (seconds)	40 characters followed by a real
12	Number of time steps	40 characters followed by an integer
13	Number of sets of results	40 characters followed by an integer
14	Generalised Crank-Nicolson parameter	40 characters followed by a real
15	Plasmapause model	40 characters followed by a string
16	Blank	
17	Name of chorus diffusion matrix	40 characters followed by a string
18	Name of hiss diffusion matrix	40 characters followed by a string
19	Name of EMIC diffusion matrix	40 characters followed by a string
20	Name of magnetosonic diffusion matrix	Not used
21	Name of lightning generated whistler diffusion matrix	Not used
22	Name of transmitter diffusion matrix	Not used
23	Type of radial diffusion diffusion coefficient	40 characters followed by a string
24	Name of collision diffusion matrix	40 characters followed by a string
25	Initial condition	40 characters followed by a string
26	Blank	
27	Title -" Pitch-angle / Energy (keV) Grid"	
28	Title - "Lshell min(energy) max(energy)"	
29 to 29+N <sub>L</sub>	L*, minimum energy, maximum energy table	Real (10 characters) real (14 characters) real (14 characters)
30+N <sub>L</sub>	Blank	
31+N <sub>L</sub>	Title	"Flux at each grid point in /(m <sup>2</sup> s sr J)"

32+N <sub>L</sub>	Blank	
33+N <sub>L</sub>	Time (seconds since the start of the run), Kp index, Plasmopause location (in L)	Title (6 characters) real (16 characters) title (8 characters) real(6 characters) title (17 characters) real (6 characters)
34+N <sub>L</sub> and following	$((Flux(i,j,k), i=0,N_\alpha) j=0,N_E) k=0,N_L)$	Ten, 12 character, real values to a line
	Blank	
	Time, Kp, Plasmopause location	As above
	$((Flux(i,j,k), i=0,N_\alpha) j=0,N_E) k=0,N_L)$	As above
	...	

717

718 Following the table of minimum and maximum energies vs L\* that starts at line 29, there are  
719 3 title lines, then the first set of output from the model. A header line gives the time in  
720 seconds since the start of the run, the Kp index at that time and the plasmopause location in  
721 L\*. This line is followed by the flux at each grid point in m<sup>-2</sup>sr<sup>-1</sup>s<sup>-1</sup>J<sup>-1</sup>, in the order  $((flux(i,j,k),$   
722  $i=0,N_\alpha) j=0,N_E) k=0,N_L)$ , i.e. with the pitch-angle index on the inner loop, the energy index on  
723 the middle loop and the L\* index on the outer loop. This array is written out 10 values to a  
724 line.

725 The flux is followed by a blank line, then the time, Kp and plasmopause position for the next  
726 set of results is given, followed by the flux again. This is repeated until the end of the run is  
727 reached.

728

729 **The .EFLUX file**

730 The format of the .EFLUX files is identical to the .3d files, except that the differential flux is  
731 replaced by differential energy flux in m<sup>-2</sup>sr<sup>-1</sup>s<sup>-1</sup>. The pitch-angle, energy and L\* grids and the  
732 timestamps will be identical to those in the corresponding .3d file and are provided for  
733 completeness.

734

735 **The .PRE file**

736 The .PRE files contain the drift-averaged, differential flux (m<sup>-2</sup>sr<sup>-1</sup>s<sup>-1</sup>J<sup>-1</sup>) at the edge of the  
737 bounce loss cone. They begin with a header with a similar format to the .3d files, but without  
738 the pitch-angle information. The header repeats some of the corresponding output in the .3d  
739 file and is there for completeness, as the output times and energy and L\* grids in the .PRE  
740 file are the same as those in the .3d file.

741 Following the table of minimum and maximum energies vs L\*, there are 3 title lines, then  
742 the first set of output from the model. The first line gives the time in seconds since the start  
743 of the run. This line is followed by the precipitating flux at each (energy, L\*) grid point in  
744 m<sup>-2</sup>sr<sup>-1</sup>s<sup>-1</sup>J<sup>-1</sup>, in the order  $((flux(j,k), j=0,N_E) k=0,N_L)$ , i.e. with the energy index on the inner loop  
745 and the L\* index on the outer loop.

746

Line	Contains	Format
1	Header	



2	Blank	
4	Maximum energy index ( $N_E$ )	40 characters followed by an integer (10 characters)
5	Maximum L* index ( $N_L$ )	40 characters followed by an integer (10 characters)
6	Minimum energy at maximum L* (keV)	40 characters followed by a real (10 characters)
7	Maximum energy at maximum L*(keV)	40 characters followed by a real (10 characters)
8	Minimum L*	40 characters followed by a real (10 characters)
9	Maximum L*	40 characters followed by a real (10 characters)
10	Start time for simulation	yyyy-mm-dd hr:mm
11	Number of sets of results	40 characters followed by an integer (10 characters)
12	Blank	
13	Title - Energy (keV) Grid	
14	Title - Lshell min Energy max Energy	
15 to 15+ $N_L$ +1	L*, minimum energy, maximum energy table	Real (10 characters) real (14 characters) real (14 characters)
15+ $N_L$ + 2	Blank	
...	Title - Precipitating flux at each grid point in /( $m^2 s sr$ )	
	Blank	
	Time	Title (6 characters) real (16 characters)
	(( $Flux(j,k), j=0,N_E$ ) $k=0,N_L$ )	Ten, 12 character, real values to a line
	Blank	
	Time	As above
	(( $Flux(i,j,k), j=0,N_E$ ) $k=0,N_L$ )	As above
	...	

747

748 The flux at the given time is followed by a blank line, then the next time is given followed by  
749 the flux again. This is repeated until the end of the run is reached.

750

751

### 752 **4.3.5 Kp prediction model**

#### 753 **Model description**

754 The geomagnetic Kp index was introduced by J. Bartels in 1949 and is derived from the  
755 standardized K index (Ks) of 13 magnetic observatories. It is designed to measure solar  
756 particle radiation by its magnetic effects and used to characterize the magnitude of  
757 geomagnetic storms. The K-index quantifies disturbances in the horizontal component of

758 Earth's magnetic field with an integer in the range 0-9 with 1 being calm and 5 or more  
759 indicating a geomagnetic storm. Kp is an excellent indicator of disturbances in the Earth's  
760 magnetic field.

761 The VSWMC contains a simple model based on the empirical equation for the least variance  
762 linear prediction of Kp proposed in the paper by Newell et al. (2008). The paper shows that  
763 Kp is highly predictable from solar wind data (even without a time history) if both a merging  
764 term and a viscous term are used. The solar wind data for the Kp prediction can be taken, for  
765 example, from EUHFORIA forecast outputs at Earth. The model calculates Kp index and  
766 outputs it as a time series file, and also draws it as a plot image.

## 767 **Model access and run information**

768 The empirical Kp prediction model is a simple Python 2.7 script that can run in the same  
769 environment as, e.g., EUHFORIA Corona. In the VSWMC framework, it is installed and run  
770 on one of the KU Leuven HPC servers, access to which is provided via ssh.

771 There are two usage modes supported by the model script.

772 • **Standalone run mode.** This runs the Kp prediction model using already available  
773 time series of solar wind parameters stored in the input file.

774 • **Coupled mode.** In this mode the Kp prediction model dynamically receives the solar  
775 wind data from another model and generates Kp index time series nearly  
776 synchronously with the other model output generation.

777 The Kp prediction model computation takes around a minute at most.

## 778 **Model input**

779 As an input Kp prediction model accepts a time series of solar wind physical parameters at  
780 Earth. The parameters required for Kp calculation are the following: particle density, velocity  
781 and magnetic field. Currently the model is implemented to take as an input the ASCII text  
782 file containing time series output of EUHFORIA Heliosphere model for Earth  
783 (`euhforia_Earth.dsv`). The file contains the following parameters:

784

<b>Output solar wind parameter</b>	<b>Data unit</b>	<b>Data type</b>
Date	YYYY-MM-DDThh:mm:ss (ISO8601 date and time format)	string
Grid point radial coordinate r	AU (Astronomical Unit)	float
Grid point colatitude clt	rad (radian)	float
Grid point longitude lon	rad (radian)	float
Number density n	1/cm <sup>3</sup> (particles per cubic centimeter)	float
Pressure P	Pa (Pascal)	float

Radial component of velocity vr	km/s (kilometers per second)	float
Colatitude component of velocity vclt	km/s (kilometers per second)	float
Longitude component of velocity vlon	km/s (kilometers per second)	float
Radial component of magnetic field Br	nT (nano Tesla)	float
Colatitude component of magnetic field Bclt	nT (nano Tesla)	float
Longitude component of magnetic field Blon	nT (nano Tesla)	float

785

786 **Model output**

787 As the output Kp prediction model generates a time series file of Kp indices. The output file  
788 name is `Kp.dat`, it is in ASCII format, and contains the following parameters:

789

Output solar wind parameter	Data unit	Data type	Accuracy
Date	YYYY-MM-DDThh:mm:ss (ISO8601 date and time format)	string	N/A
Kp index	dimensionless	float	1 decimal place

790

791 The model also generates the Kp index plot image as the output with the name  
792 `Earth_plot_kp.png`.

793

794 **4.3.6 Dst prediction model**

795 **Model description**

796 The Dst or disturbance storm time index is a measure of geomagnetic activity used to assess  
797 the severity of magnetic storms. It is expressed in nanoteslas (nT) and is based on the average  
798 value of the horizontal component of the Earth's magnetic field measured hourly at four  
799 near-equatorial geomagnetic observatories. Use of the Dst as an index of storm strength is  
800 possible because the strength of the surface magnetic field at low latitudes is inversely  
801 proportional to the energy content of the ring current, which increases during geomagnetic  
802 storms. In the case of a classic magnetic storm, the Dst shows a sudden rise, corresponding  
803 to the storm sudden commencement, and then decreases sharply as the ring current  
804 intensifies. Once the IMF turns northward again and the ring current begins to recover, the

805 Dst begins a slow rise back to its quiet time level. The relationship of inverse proportionality  
806 between the horizontal component of the magnetic field and the energy content of the ring  
807 current is known as the Dessler-Parker-Sckopke relation. Other currents contribute to the  
808 Dst as well, most importantly the magnetopause current. The Dst index is corrected to  
809 remove the contribution of this current as well as that of the quiet-time ring current.

810 The VSWMC contains a simple model based on the empirical equation for Dst prediction  
811 proposed in the paper by O Brien and McPherron (2000). The paper uses a large database  
812 of ring current and solar wind parameters, covering hundreds of storms. Any study of  
813 individual storms is highly susceptible to the uncertainty inherent in the Dst index. The  
814 paper shows, however, that the empirical Burton equation, with only slight modification,  
815 does accurately describe the dynamics of the ring current index Dst. That is, allowing the  
816 decay time to vary with interplanetary electric field VBs is the only modification necessary.

817 The solar wind data for the Dst prediction can be taken, for example, from EUHFORIA  
818 forecast outputs at Earth. Initial Dst value required for correct index calculation is taken  
819 from the ODI `index_dst.dst` dataset. The model calculates Dst index and outputs it as a  
820 time series file, and also draws it as a plot image.

## 821 **Model access and run information**

822 The empirical Dst prediction model is a simple Python 2.7 script that can run in the same  
823 environment as, e.g., EUHFORIA Corona. In the VSWMC framework, it is installed and run  
824 on one of the KU Leuven HPC servers, access to which is provided via ssh.

825 There are two usage modes supported by the model script.

- 826 • **Standalone run mode.** This runs the Dst prediction model using already available  
827 time series of solar wind parameters stored in the input file.
- 828 • **Coupled mode.** In this mode the Dst prediction model dynamically receives the  
829 solar wind data from another model and generates Dst index time series nearly  
830 synchronously with the other model output generation.

831 The Dst prediction model computation takes around a minute at most.

## 832 **Model input**

833 As an input Dst prediction model accepts a time series of solar wind physical parameters at  
834 Earth and an initial Dst value required by the model for correct index calculation. The  
835 parameters required for Dst calculation are the following: particle density, velocity and  
836 magnetic field. Currently the model is implemented to take as an input the ASCII text file  
837 containing time series output of EUHFORIA Heliosphere model for Earth  
838 (`euhforia_Earth.dsv`). The file contains the following parameters:

839

<b>Input solar wind parameter</b>	<b>Data unit</b>	<b>Data type</b>
Date	YYYY-MM-DDThh:mm:ss (ISO8601 date and time format)	string

Grid point radial coordinate r	AU (Astronomical Unit)	float
Grid point colatitude clt	rad (radian)	float
Grid point longitude lon	rad (radian)	float
Number density n	1/cm <sup>3</sup> (particles per cubic centimeter)	float
Pressure P	Pa (Pascal)	float
Radial component of velocity vr	km/s (kilometers per second)	float
Colatitude component of velocity vclt	km/s (kilometers per second)	float
Longitude component of velocity vlon	km/s (kilometers per second)	float
Radial component of magnetic field Br	nT (nano Tesla)	float
Colatitude component of magnetic field Bclt	nT (nano Tesla)	float
Longitude component of magnetic field Blon	nT (nano Tesla)	float

840

841 The initial Dst value is taken during the model start-up by sending a query to the ODI  
842 database with the use of a php script.

### 843 **Model output**

844 As the output Dst prediction model generates a time series file of Dst indices. The output file  
845 name is `Dst.dat`, it is in ASCII format, and contains the following parameters:

846

<b>Output solar wind parameter</b>	<b>Data unit</b>	<b>Data type</b>	<b>Accuracy</b>
Date	YYYY-MM-DDThh:mm:ss (ISO8601 date and time format)	string	N/A
Dst index	nT (nano Tesla)	float	5 decimal places

847

848 The model also generates the Dst index plot image as the output with the name  
849 `euHfonia_Earth_plot_dst.png`.

850

851

852 **4.3.7 Magnetopause standoff distance model**

853 **Model description**

854 The magnetopause is the boundary between the magnetic field of the planet and the solar  
855 wind. The location of the magnetopause is determined by the balance between the pressure  
856 of the planetary magnetic field and the dynamic pressure of the solar wind.

857 This document describes a simple model for the prediction of the standoff distance from the  
858 Earth to the magnetopause along the line to the Sun based on the equation proposed in the  
859 Shue model (Taktakishvili et al. 2009). To improve predictions under extreme solar wind  
860 conditions the Shue model takes into consideration a nonlinear dependence of the  
861 parameters on the solar wind conditions to represent the saturation effects of the solar wind  
862 dynamic pressure on the flaring of the magnetopause and saturation effects of the  
863 interplanetary magnetic field  $B_z$  on the subsolar standoff distance.

864 The solar wind data for the magnetopause standoff distance prediction can be taken, for  
865 example, from EUHFORIA forecast outputs at Earth. The model calculates magnetopause  
866 standoff distance and outputs it as a time series file, and also draws it as a plot image.

867 **Model access and run information**

868 The magnetopause standoff distance prediction model is a simple Python 2.7 script that can  
869 run in the same environment as, e.g., EUHFORIA Corona. In the VSWMC framework, it is  
870 installed and run on one of the KU Leuven HPC servers, access to which is provided via ssh.

871 There are two usage modes supported by the model script.

- 872 • **Standalone run mode.** This runs the magnetopause standoff distance prediction  
873 model using already available time series of solar wind parameters stored in the input  
874 file.
- 875 • **Coupled mode.** In this mode the magnetopause standoff distance prediction model  
876 dynamically receives the solar wind data from another model and generates  
877 magnetopause standoff distance time series nearly synchronously with the other  
878 model output generation.

879 The magnetopause standoff distance prediction model computation takes around a minute  
880 at most.

881 **Model input**

882 As an input magnetopause standoff distance prediction model accepts a time series of solar  
883 wind physical parameters at Earth. The parameters required for magnetopause standoff  
884 distance calculation are the following: particle density, velocity and magnetic field. Currently  
885 the model is implemented to take as an input the ASCII text file containing time series output  
886 of EUHFORIA Heliosphere model for Earth (`euhforia_Earth.dsv`). The file contains the  
887 following parameters:

888

Output solar wind parameter	Data unit	Data type
-----------------------------	-----------	-----------

Date	YYYY-MM-DDThh:mm:ss (ISO8601 date and time format)	string
Grid point radial coordinate r	AU (Astronomical Unit)	float
Grid point colatitude clt	rad (radian)	float
Grid point longitude lon	rad (radian)	float
Number density n	1/cm <sup>3</sup> (particles per cubic centimeter)	float
Pressure P	Pa (Pascal)	float
Radial component of velocity vr	km/s (kilometers per second)	float
Colatitude component of velocity vclt	km/s (kilometers per second)	float
Longitude component of velocity vlon	km/s (kilometers per second)	float
Radial component of magnetic field Br	nT (nano Tesla)	float
Colatitude component of magnetic field Bclt	nT (nano Tesla)	float
Longitude component of magnetic field Blon	nT (nano Tesla)	float

889

890 **Model output**

891 As output magnetopause standoff distance prediction model generates a time series file of  
892 magnetopause standoff distances. The output file name is `DSO.dat`, it is in ASCII format,  
893 and contains the following parameters:

894

<b>Output solar wind parameter</b>	<b>Data unit</b>	<b>Data type</b>	<b>Accuracy</b>
Date	YYYY-MM-DDThh:mm:ss (ISO8601 date and time format)	string	N/A
Magnetopause standoff distance	Re	float	1 decimal place

895

896 The model also generates the magnetopause standoff distance plot image as the output with  
897 the name `Earth_plot_dso.png`.

898

### 899 **4.3.8 ODI**

#### 900 **Model description**

901 The main data source for commonly used datasets (such as solar wind parameters, IMF  
902 parameters, magnetic indices) is an Open Data Interface instance maintained at  
903 ESA/ESTEC. ODI is a database framework which allows for streamlined data downloads and  
904 ingestion (<https://spitfire.estec.esa.int/trac/ODI/wiki/ODIv5>). The ESTEC instance is  
905 accessible through a REST interface for data queries.

906 In order to integrate access to the ODI database into the VSWMC framework, a php script  
907 was written that formulates REST requests, executes them and outputs the download data  
908 into a flat ASCII file. For all intents and purposes, the php script can be considered to be a  
909 model federate which provides inputs for model runs and as such can be coupled to other  
910 federates.

911 A secondary php script was added to retrieve the start and end epochs of a (set of) dataset(s).

#### 912 **Model access and run information**

913 The ODI federate is instantiated as a single php script (`runODI.php`) which is to be run on  
914 command line with a number of named parameters to specify the time range, data cadence,  
915 and a list of quantities to be retrieved. No other modules need to be loaded in order to execute  
916 the php script. Access to the ESA/ESTEC ODI server at <https://spitfire.estec.esa.int/> should  
917 be allowed in the firewall rules (standard https port).

#### 918 **Model input**

919 All model inputs are supplied as named parameters in a command line call.

#### 920 **Model output**

921 At present, ODI is used as a data provision tool for a small (but growing) number of federates,  
922 e.g. GUMICS or the BAS RBM model. The quantities required are specific to each model, and  
923 as such it is not possible to provide a definitive list of output quantities for the ODI federate.  
924 However, the SPASE SimulationModel file for ODI contains all information (e.g. physical  
925 units, coordinate systems) on the quantities that can currently be retrieved from the ODI  
926 database. When additional quantities are added in future, the SPASE file will be updated as  
927 well.

928

### 929 **4.3.9 Visualization ‘federate’**

#### 930 **Model description**

931 The purpose of the Visualization federate is to automatically generate 2D/3D images or  
932 movies showcasing the evolution of a simulation using tools like Python Matplotlib,  
933 Paraview, Visit (all open source), or Tecplot, IDL (commercial), etc. The users will be able to



934 view these images/movies via the web interface. Those 2D/3D images and movies will offer  
935 a preview of the simulation results, since the end-user will be able to download the full  
936 simulation output data sets to his/her own computer for offline visualization and use tools  
937 like Paraview, Visit, or Tecplot, as long as the file format is compatible to those software  
938 packages. It is also possible to use Visualization federate for conversion of the original model  
939 output file formats to the formats compatible with the offline visualization tools, and make  
940 them available for downloading, using special tools, utilities, or scripts provided with the  
941 models for this purpose.

942 The VSWMC contains a Visualization federate for the EUHFORIA Heliosphere simulation  
943 output visualization based on the Python script provided together with the model. The script  
944 processes the EUHFORIA Heliosphere output files and generates two 2D images (for the  
945 solar wind particle density and radial velocity components) for each of the model output  
946 cycle. Using these images the VSWMC GUI component creates an animated slide show  
947 available via the web interface.

#### 948 **Model access and run information**

949 The Visualization federate uses the EUHFORIA Heliosphere visualization script as a model,  
950 which is a simple Python 2.7 script that can run in the same environment as, e.g., EUHFORIA  
951 Corona. In the VSWMC framework, it is installed and run on one of the KU Leuven HPC  
952 servers, access to which is provided via ssh.

953 There are two usage modes supported by the model script.

- 954 • **Standalone run mode.** This runs the EUHFORIA Heliosphere visualization script  
955 using already available (pre-generated) model output files with solar wind data.
- 956 • **Coupled mode.** In this mode the Visualization federate dynamically receives solar  
957 wind data files during the EUHFORIA Heliosphere run and generates images nearly  
958 synchronously with the model output generation. The federate runs the visualization  
959 script each time the model generates new output files.

960 The visualization script computation takes around a minute.

#### 961 **Model input**

962 As an input the visualization script accepts the EUHFORIA Heliosphere output data saved  
963 in binary files in the NumPy format (NPY, NPZ) for the whole simulation period. An NPZ  
964 (NumPy Zipped Data) file contains NPY files with particular physical parameter data each.  
965 An NPY file is named after the parameter it contains, e.g.: `Br.npy`, or `vclt.npy`. The files  
966 contain the physical parameters of solar wind from 21.5 Rs to 2 AU (or further if necessary).  
967 The parameters are the following:

<b>Output solar wind parameter</b>	<b>Data unit</b>	<b>Data type</b>
Date	YYYY-MM-DDThh:mm:ss (ISO8601 date and time format)	string

Grid point radial coordinate r	AU (Astronomical Unit)	float
Grid point colatitude clt	rad (radian)	float
Grid point longitude lon	rad (radian)	float
Number density n	1/cm <sup>3</sup> (particles per cubic centimeter)	float
Pressure P	Pa (Pascal)	float
Radial component of velocity vr	km/s (kilometers per second)	float
Colatitude component of velocity vclt	km/s (kilometers per second)	float
Longitude component of velocity vlon	km/s (kilometers per second)	float
Radial component of magnetic field Br	nT (nano Tesla)	float
Colatitude component of magnetic field Bclt	nT (nano Tesla)	float
Longitude component of magnetic field Blon	nT (nano Tesla)	float

968

## 969 **Model output**

970 The visualization script outputs two 2D images: for solar wind particle density and radial  
971 velocity component. Each image consists of three parts that plot corresponding parameter  
972 distribution in the constant Earth latitude plane, the meridional plane of the Earth and the  
973 parameter time series profile at Earth.

974

975 The solar wind particle density plot is named as following: `n_scaled_YYYY-MM-DDTHH-MM-`  
976 `SS.png`, where `YYYY-MM-DDTHH-MM-SS` corresponds to the time stamp of the input file,  
977 and the radial velocity plot is named as following: `vr_YYYY-MM-DDTHH-MM-SS.png`.

978

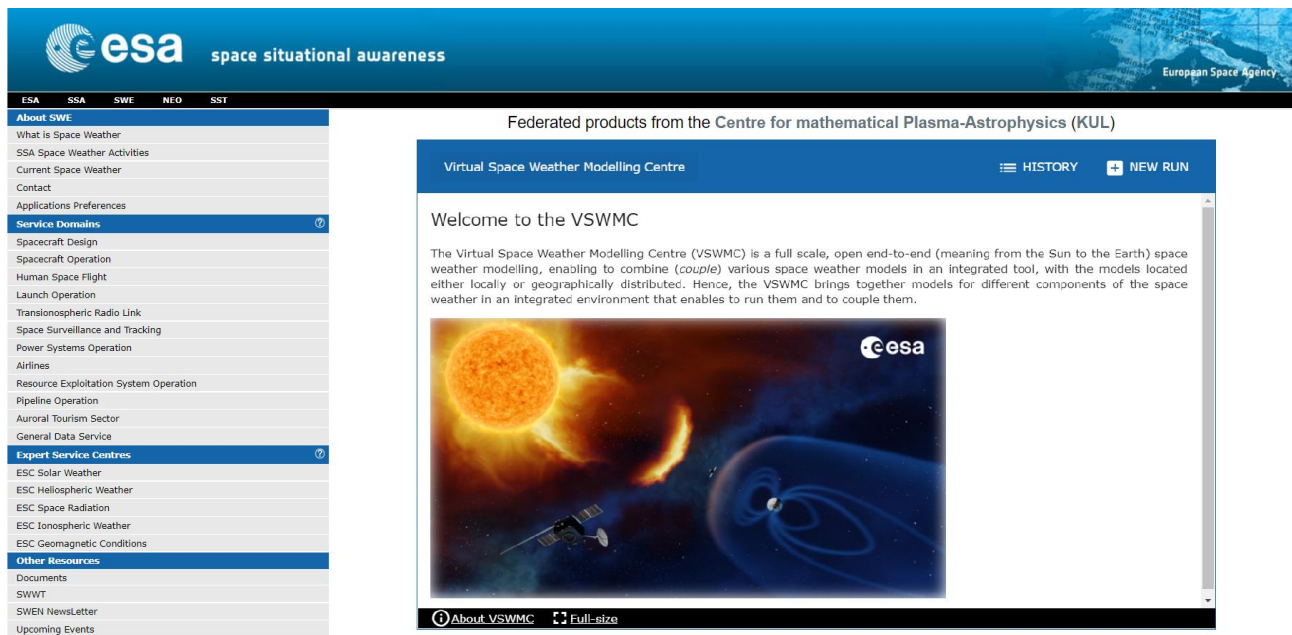
## 979 **4.4 Development of Data provision nodes**

980

981 The ODI script (see Section 4.3.8) has been extended and supplemented with additional  
982 supporting scripts. For instance, it now enables OMNI data (spacecraft-interspersed, near-  
983 Earth solar wind data) input that is used for COOLFluid, GUMICS4 and as input for the  
984 magneto pause stand-off distance (used for BAS-RBM). Other additional data sources  
985 include GOES and ACE near-real time data of the solar wind, interplanetary magnetic field  
986 (IMF) and electron and proton radiation environment in GEO.

987  
988  
989  
990  
991  
992  
993  
994  
995

Other external datasets have also been exploited in the new VSWMC system. EUHFORIA Corona, for instance, uses magnetograms from the Global Oscillation Network Group (GONG) database, and the cone CME parameters for the EUHFORIA Heliosphere model are retrieved from the Space Weather Database Of Notifications, Knowledge, Information (DONKI) server which has been developed at the Community Coordinated Modeling Center (CCMC).



996  
997  
998  
999

**Figure 6:** Mock-up of screen shot of the VSWMC welcome page once integrated in the SSA SWE Portal providing an impression of how the integrated VSWMC will look.

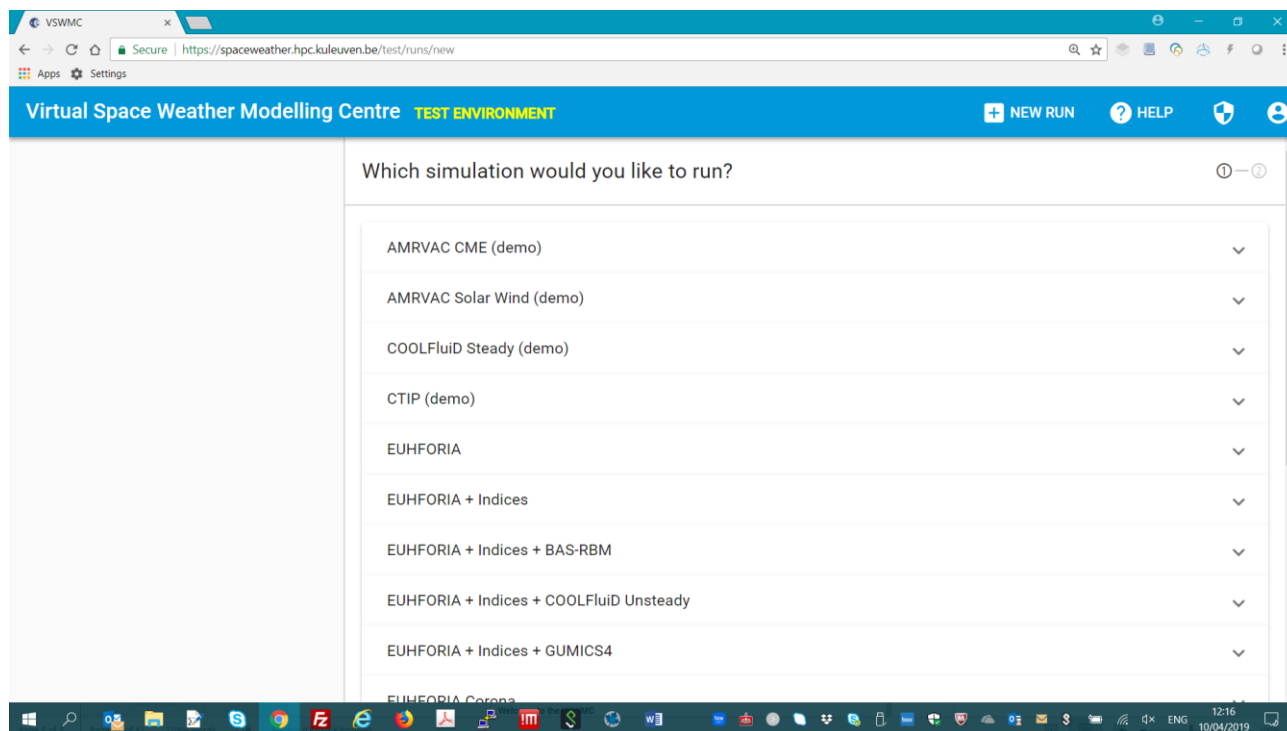
1000  
1001

## 1002 **4.5 Running models and coupled models via the User Front-End** 1003 **(GUI)**

1004 As not all models integrated in the VSWMC are sufficiently mature yet, the mature models  
1005 and model couplings have been duplicated in a limited (but operational) system (with  
1006 another URL: <https://spaceweather.hpc.kuleuven.be/>, accessible via the H-ESC webpage as  
1007 described above). [Figure 6](#) shows how the VSWMC welcome page looks when integrated in  
1008 the SSA SWE Portal. This limited system passed the acceptance tests for integration in the  
1009 H-ESC and has been made available to a user community (cf. Section 4.3). The full  
1010 development system will be maintained in the same time, of course. Clicking on the **NEW RUN**  
1011 button in the upper banner on the right, one gets a list of all currently available models  
1012 (including the demo models) and model couplings, as shown in [Figure 7](#). The same action in  
1013 the operational system gives a more limited list of models and model couplings as the  
1014 immature 'demo' models and couplings are not listed there. But as apart from that both  
1015 systems are identical, including the info pages.

1016 When clicking on one of the offered federates, the actual set up is depicted showing all the  
1017 models involved. This is demonstrated in the screen shot below (Figure 8) for the  
1018 EUHFORIA + indices option. Hence, it is immediately clear that this model chain involves 6  
1019 federates, viz. EUHFORIA Corona and EUHFORIA Heliosphere, the Visualizer of  
1020 EUHFORIA results, and three empirical geo-effective index models that use the synthetic  
1021 solar wind data at L1 from EUHFORIA to determine the Kp and Dst indices and the  
1022 magnetopause standoff distance.

1023



1024  
1025

1026

**Figure 7:** Choice offered when requesting a new run (in the test environment system).

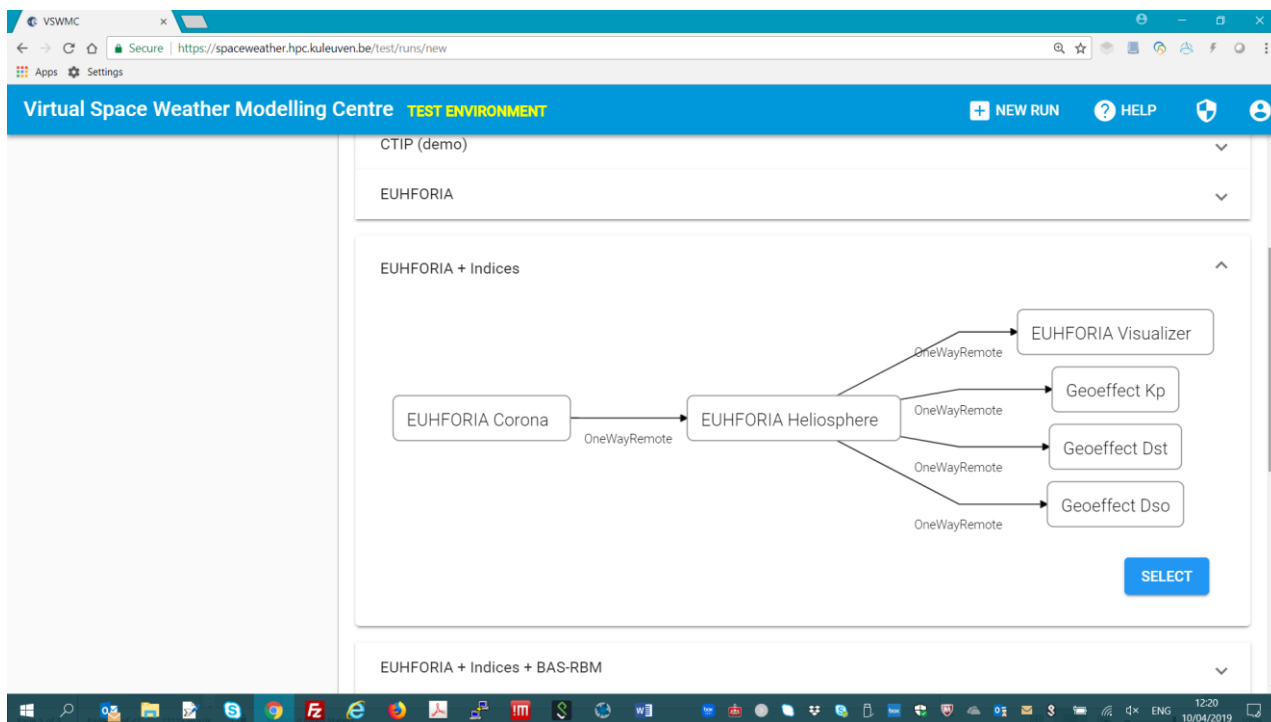
1027

1028 Upon selecting the model or model chain, the GUI displays the input page offering different  
1029 options for all the input required to successfully run the coupled models. As soon as the  
1030 minimum required input is available, the ‘Start the run’ button lights up, indicating the  
1031 model could run with the provided input. At this point the input can still be modified or  
1032 complimented, e.g. by adding CMEs, or changing the CME parameters for the EUHFORIA  
1033 Heliospheric evolution model. When the ‘Start the run’ button is pushed, the simulation  
1034 starts and the user sees the log screen enabling him to follow the status of the different  
1035 models in the chain. The model or model chain is shown in the left column in orange, with  
1036 an indication on how long it has been running.

1037

1038 When the simulation is finished, the model or chain in the left column turns green. Clicking  
1039 on it, show all the runs made by the user with this specific model, indicating which runs were  
1040 successful, or stopped (by the user) or unsuccessful, see Figure 9 below. The most recent run  
1041 is on top of the list. Clicking on it triggers the GUI to show the page for this specific  
1042 simulation run, which contains tabs with the input parameters, the log screen and the

1043 results. These consist of output files (e.g. the solar wind parameters at Earth, Stereo A,  
1044 Mars and other planets or even virtual satellites) and, if applicable, visualizations (plots and  
1045 movies). All these files can be previewed and/or downloaded by simply clicking on the  
1046 appropriate buttons behind the file names. As an example, we show in [Figure 10](#) one of the  
1047 145 snapshots of the radial velocity in the equatorial and meridional planes from the movie  
1048 produced for the EUHFORIA chain run.  
1049  
1050



1051

1052

1053

**Figure 8:** the EUHFORIA + indices model chain.

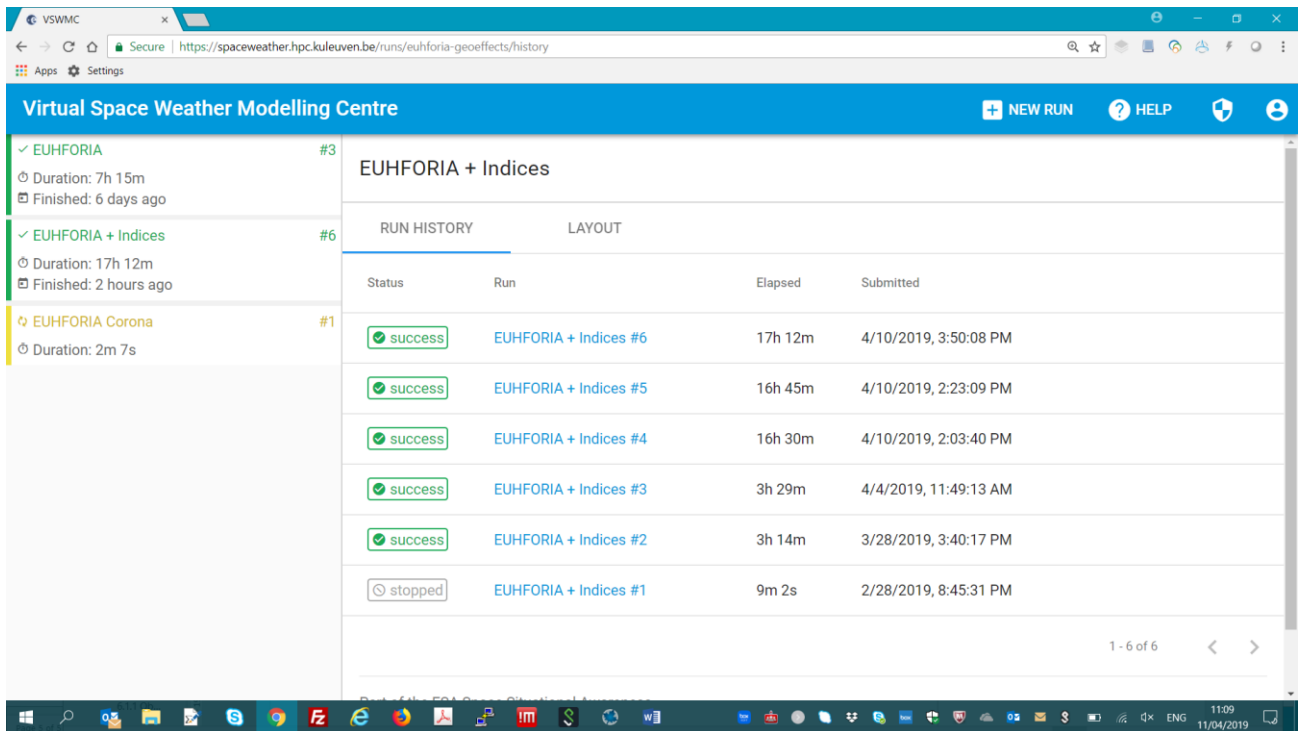


Figure 9: Example of list of runs made with a certain model or model chain (in this case EUHFORIA + indices).

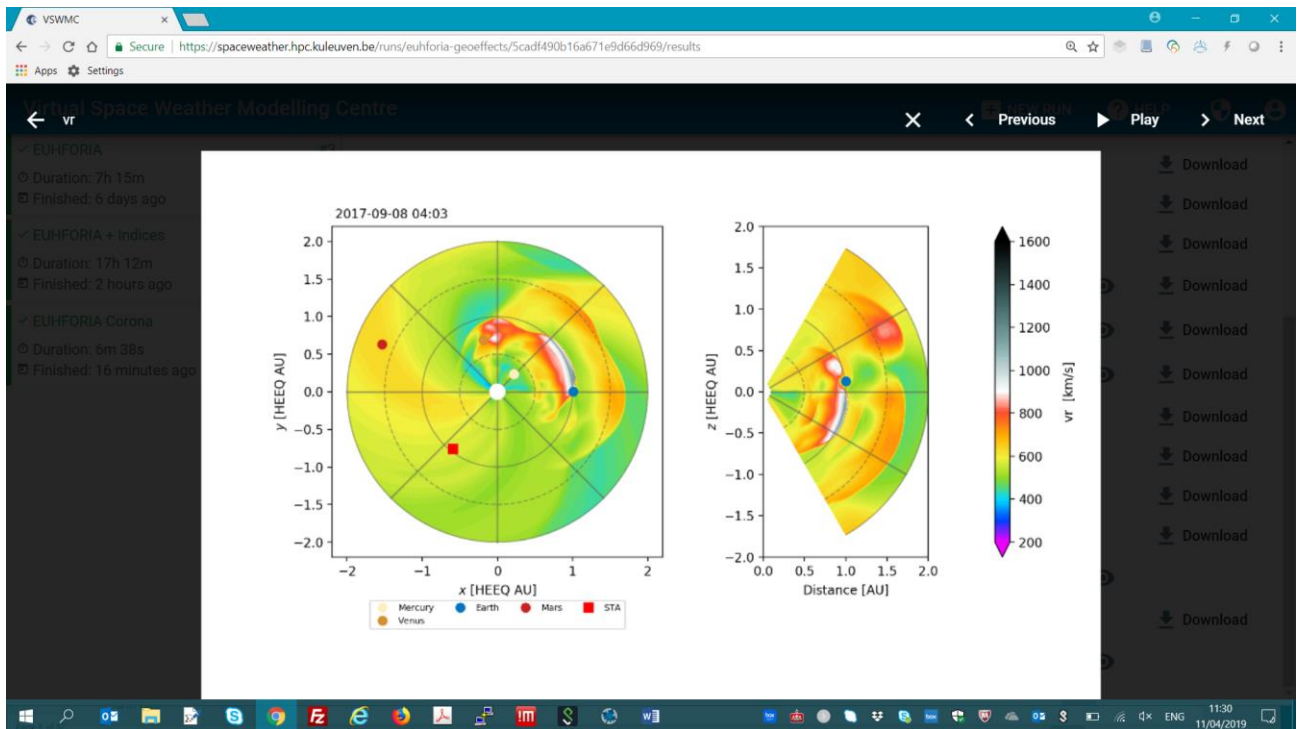


Figure 10: Example screenshot of the radial velocity in the equatorial plane (left) and meridional plane of the Earth (right).

1062

## 5 FUNCTIONALITY OF THE SYSTEM

1063

1064

1065

1066

1067

1068

1069

1070

1071

1072

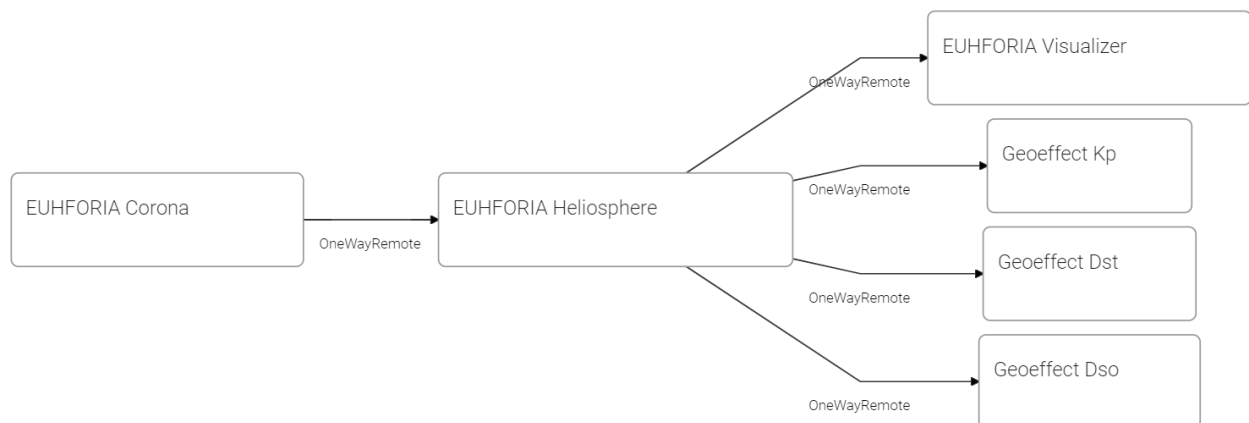
1073

1074

1075

1076

A set of HLA federations (coupled simulations) has been deployed in the VSWMC, including several end-to-end chain of existing physics-based models. For instance, the coupling of EUHFORIA Corona – EUHFORIA Heliosphere – EUHFORIA Visualizer, combines three federates and first calculates the Wang-Sheeley-Arge corona using a GONG magnetogram uploaded from the external GONG database, and yields the MHD parameters at 0.1 AU which are used as boundary conditions for the Heliospheric wind on which cone CMEs can be superposed. The parameters of the latter can be typed in or uploaded from another external (DONKI) database. The output files of the time dependent 3D MHD simulation are turned into standard plots and movies by the visualization federate. The model chain EUHFORIA Corona – EUHFORIA Heliosphere – EUHFORIA Visualizer + the three geo-effect indices models (Dst index, Kp index and magnetopause stand-off distance), see [Fig. 11](#), does the same as the previous one but computes on top of that the Kp and Dst indices and the magnetopause stand-off distance from the (synthetic) solar wind parameters at L1.



1077

1078

**Figure 11:** EUHFORIA coupled to the geo-effect indices models.

1079

1080

1081

1082

1083

1084

1085

1086

The next model chain depicted in in [Figure 12](#) also involves 7 federates but is slightly more complicated and involves also the BAS-RBM model. In fact, the output of EUHFORIA is used to calculate the Kp index and this is subsequently used as one of the inputs for the BAS Radiation Belt models. The other required input for BAS-RBM is also synthetic in this example and taken from the magnetopause stand-off distance model that is supplied itself with synthetic wind data at L1 from EUHFORIA.

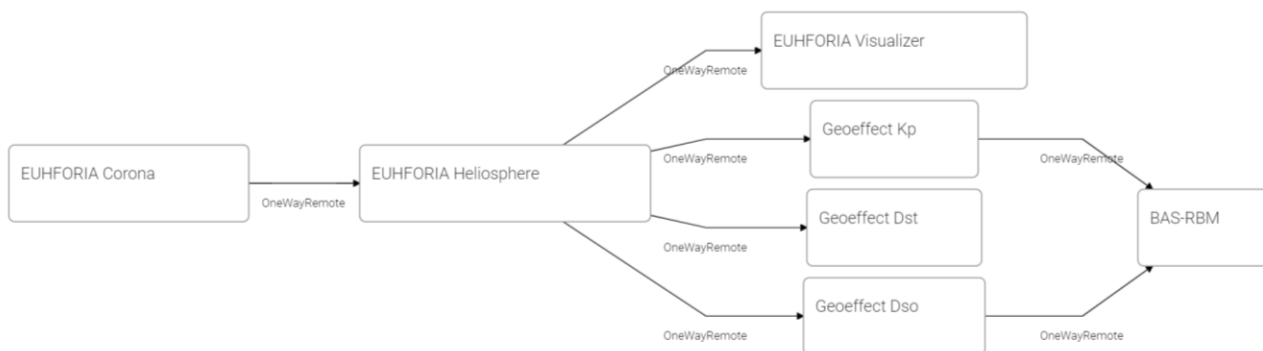


**Figure 12:** The BAS-RBM model in a model chain such that it can be fed with synthetic Kp and magnetopause stand-off distance data obtained from solar wind parameters calculated by EUHFORIA.

1087  
1088  
1089  
1090

1091

## 1092 **6 LESSONS LEARNED AND FUTURE DEVELOPMENT**

### 1093 **6.1 Challenges and lessons learned**

1094 The development and especially the verification and validation tests have revealed several  
1095 challenges for the VSWMC, including:

- 1096 • It turned out to be difficult to convince the modellers to provide their models, even  
1097 though the compiled object files suffice, and to fill out the necessary ICD forms, even  
1098 though this is not a big work load. Without the information in the ICD form, however,  
1099 it turned out to be extremely difficult to install the model and to adjust the GUI to run  
1100 the model.
- 1101 • CPU capacity: some of the models are 3D time dependent and require a lot of CPU  
1102 time to run. These are installed on a computer cluster which is not dedicated, i.e. also  
1103 used by others. But even if the cluster would be a dedicated one, the fact that multiple  
1104 users exploit the system simultaneously means that the cluster must be operated as a  
1105 batch system. This means that the simulations are queued and run one after the other,  
1106 or simultaneously if there are sufficient nodes available;
- 1107 • Data storage: some of the models generate a huge amount of data. These data cannot  
1108 be stored forever and it will have to be decided which data are kept and which erased  
1109 after 2-3 weeks;
- 1110 • Wall clock time: some models are not parallel, e.g. GUMICS4, which means they run  
1111 on a single processor and this can take a lot of time. For GUMICS4 with 5 levels of  
1112 adaptation of the grid, the wall clock time is an order of magnitude longer than real  
1113 time. This can only be solved by installing a parallel version of the model;
- 1114 • Network: Running the models requires a lot of communication between the VSWMC  
1115 system server and the (remote) clusters on which the models are installed. When there  
1116 are interruptions of these communications, it is a challenge to retrieve the links. The  
1117 tests revealed that sometimes the model ran successfully, but due to loss of the link,  
1118 the user could not see that;



- 1119 • Two-way couplings remain a challenge, especially if the two models are not installed  
1120 in the same location.

1121 We did check different levels of model integration. For instance, the XTRAPOL model runs  
1122 in Paris and the cluster there has been integrated as a full VSWMC node. The BAS-RBM  
1123 model, however, is integrated at the lowest possible level: the input is generated by the  
1124 VSWMC and placed in a folder at BAS where the system checks once per minute if an input  
1125 file is provided. If so, it runs the BAS-RBM with this input file and puts the output in another  
1126 folder. The VSWMC automatically checks whether the output files are available and  
1127 downloads them to the VSWMC if necessary. This is a delicate setup that slows down coupled  
1128 simulations and enables only a weak couplings to other models in the system. But it works,  
1129 at least for simple couplings in which the models run in series and not simultaneously, and  
1130 as long as the weakly coupled model is at the end of the model chain. It remains to be tested  
1131 whether this setup also works for a model in the middle of a chain.

1132

## 1133 **6.2 Future updates and development**

1134 Part 3 of the VSWMC should address the above-mentioned challenges and also make the  
1135 system ‘idiot proof’, i.e. verify automatically if the given parameter values are within a  
1136 physically meaningful range, or prevent the possibility to provide ‘unphysical’ values.

1137 The system could also make an estimate of the required CPU time and data storage a specific  
1138 run of a model or a model chain will require. Although the system makes it very simple to set  
1139 up simulations, the users not always realize how much they ask from the back-end system  
1140 by requesting a run or a set of runs.

1141 Another improvement would be automatic checks of all components of the system that can  
1142 be run when a new model has been added or a new coupling has been established or a model  
1143 has been changed, as this might influence the system in unexpected manners. An update of  
1144 a model might for instance ruin all model chains in which that particular mode features. Or  
1145 even an upgrade of a compiler of the cluster on which a model is installed may ruin the  
1146 simulation runs in which that model is involved.

1147 The Part 2 system does not deliver any hardware platform but rents computing and storage  
1148 resources from KU Leuven via a virtual server and runs the simulations on one of the  
1149 available clusters at KU Leuven and the clusters in graphically distributed nodes, like at VKI  
1150 (Sint-Genesius-Rode), in Paris (École Polytechnique) and Cambridge (BAS). Given the  
1151 uncertainties of the growth rate of the model, data and simulation repositories of the  
1152 VSWMC-P2 system, the number of the different types of users, and the actual demand of  
1153 CPU time, computer memory and data storage, we recommend that ESA follows this strategy  
1154 for at least a few years, in order to keep the flexibility of the system and to perform a  
1155 scalability analysis of the entire system setup.

1156 Future Run-Time System (RTS) functionality might include more flexibility. For instance,  
1157 models may run on different nodes and the RTS could find out which node will provide the  
1158 fastest execution for a particular simulation, depending on the capacity and use of the  
1159 different nodes in the system. Alternatively, some models might be executed in the Cloud. It  
1160 may even become possible to execute large parallel simulations simultaneously on different  
1161 clusters. The latter would be feasible even with today’s technology for ensemble simulations

1162 as these are ‘embarrassingly parallel’ and can simply run the same simulation model with  
1163 different sets of input parameters in parallel on different nodes of the same cluster or on  
1164 different clusters, depending on the availability and level of usage of the different clusters in  
1165 the system.

1166 For the prototype, the Developer Environment consists of simple scripts that can be used to  
1167 create/validate/upload models. It is expected that this procedure will be used for a while  
1168 until it will become clearer whether a more integrated development environment is actually  
1169 needed or not.

1170 In the future, many more models and model chains, like those in the current VSWMC-P2  
1171 system, need to be established. The list of models integrated into the VSWMC thus needs to  
1172 be expanded, including more data streams, alternative CME evolution models (e.g. the Drag-  
1173 Based Model), CME onset models (e.g. XTRAPOL), ionosphere and thermosphere models,  
1174 SEP acceleration and transport models, alternative global coronal models, etc. In particular,  
1175 the SEP transport models, that need a combined global MHD coronal model and MHD  
1176 heliospheric wind and CME evolution model as input, would profit from the VSWMC setup.

1177 To increase the awareness of the modellers on the usability of VSWMC we suggest to setup  
1178 demo sessions, e.g. during the Fair on the European Space Weather Week, to demonstrated  
1179 the easiness of use and the possibilities and potential of the VSWMC. On such occasions, it  
1180 could also be clarified with examples, how easy it is to include a new model and to provide  
1181 the necessary information via the ICD form, providing a template ICD and some examples.

## 1182 **7 SUMMARY AND CONCLUSION**

1183 The VSWMC-P2 consortium succeeded in extending the VSWMC Phase 1 prototype by  
1184 implementing a graphical user interface (GUI), facilitating the operation; providing a  
1185 generalized framework implementation; including full-scale models that can easily be run  
1186 via the GUI; including more and more complicated model couplings; including several  
1187 visualization models; creating a modest operational system that has been integrated into the  
1188 SSA SWE service network and is thus accessible via the SWE portal.

1189  
1190 In conclusion, the VSWMC system has been successfully integrated into the SWE network  
1191 as a federated SWE service at level 2 integration which required that a remote website  
1192 integrates the SWE Portal’s Identity and Single Sign-on (SSO) subsystem, making it available  
1193 via its home institute, and federated as part of the product portfolio of the Heliospheric  
1194 Weather ESC. We succeeded in extending the VSWMC prototype substantially by a complete  
1195 redesign of the core system, implementing a graphical user interface (GUI), including full-  
1196 scale models that can easily be run via the GUI, including more and more complicated model  
1197 couplings involving up to 7 different models, some of which are ready for operational use,  
1198 and also including several visualization models that can be coupled to the models so that  
1199 standard output pictures and movies are automatically generated, and which can be viewed  
1200 directly via the GUI and downloaded.

1201  
1202 The new VSWMC has great potential to add value to ESA's SSA SWE service network, even  
1203 though the amount of models integrated is limited and some of these models are only demo  
1204 versions. Full support of the modellers is often needed for a proper integration in the system,  
1205 especially when the model needs to be coupled to other models. However, it is expected that

1206 modellers will want to participate in the VSWMC and provide their model once the system  
1207 gets operational and the many advantages will become apparent.

1208

### 1209 **Acknowledgements**

1210 These results were obtained in the framework of the ESA project "SSA-P2-SWE-XIV - Virtual  
1211 Space Weather Modelling Centre - Phase 2" (ESA Contract No. 4000116641/15/DE-MRP,  
1212 2016-2019). Additional support from the projects C14/19/089 (C1 project Internal Funds  
1213 KU Leuven), G.OA23.16N (FWO-Vlaanderen), C~90347 (ESA Prodex), Belpo BRAIN  
1214 project BR/165/A2/CCSOM and EU H2020-SPACE-2019 (SU-SPACE-22-SEC-2019 –  
1215 Space Weather) project "EUHFORIA 2.0" is greatly acknowledged. For the computations we  
1216 used the infrastructure of the VSC – Flemish Supercomputer Center, funded by the Hercules  
1217 foundation and the Flemish Government – department EWI.

1218

1219

### 1220 **Bibliography**

1221 Amari, T., T. Z. Boulmezaoud, and J. J. Aly. Well posed reconstruction of the solar coronal magnetic field.  
1222 *Astron. & Astrophys.*, **446**, 691-705, 2006, DOI: 10.1051/0004-6361/20054076

1223

1224 Eastwood, J.P., E. Biffis, M. A. Hapgood, L. Green, M.M. Bisi, R.D. Bentley, R. Wicks, L.-A. McKinnell, M.  
1225 Gibbs, and C. Burnett. The Economic Impact of Space Weather: Where Do We Stand? **Risk Analysis**, Vol.  
1226 **37** (2), 206-218, 2017, DOI: 10.1111/risa.12765

1227

1228 ESA SSA Team. Space Situational Awareness – Space Weather Customer Requirements Document (CRD).  
1229 SSA-SWE-RS-CRD-1001, issue 4.5a, 28/07/2011. Available at <http://swe.ssa.esa.int/documents>

1230

1231 Fuller-Rowell, T.J., and D. Rees. A three-dimensional time-dependent global model of the thermosphere. *J.*  
1232 *Atmos. Sci.*, **37**, 2545–2567, 1980, DOI: 10.1175/1520-0469(1980)037<2545:ATDTDG>2.0.CO;2

1233

1234 Glauert, S., R. Horne, and N. Meredith. Three dimensional electron radiation belt simulations using the BAS  
1235 Radiation Belt Model with new diffusion models for chorus, plasmaspheric hiss and lightning-generated  
1236 whistlers. *Journal of Geophysical Research: Space Physics*, **119**. 268-289, 2014, DOI: 10.1002/2013JA019281

1237

1238 Harvey, J. W., et al., The Global Oscillation Network Group (GONG) project. *Science*, **272** (5266), 1284–1286  
1239 (1996), DOI: 10.1126/science.272.5266.1284

1240

1241 Hosteaux, S., E. Chané, B. Decraemer, D. Tălpeanu, and S. Poedts. Ultra-high resolution model of a breakout  
1242 CME embedded in the solar wind. *Astron. & Astrophys.*, **620**, A57 (2018), DOI: 10.1051/0004-  
1243 6361/201832976

1244

1245 Hosteaux, S., E. Chané, and S. Poedts. On the effect of the solar wind density on the evolution of normal and  
1246 inverse Coronal Mass Ejections. *Astron. & Astrophys.*, accepted, in press AA/2019/35894 (2019).

1247

1248 Janhunen, P., M. Palmroth, T. Laitinen, I. Honkonen, L. Juusola, G. Facskó, and T. Pulkkinen. The GUMICS-  
1249 4 global MHD magnetosphere–ionosphere coupling simulation, *J. Atmos. Sol.-Terr. Phys.*, **80**, 48–59, 2012,  
1250 DOI: 10.1016/j.jastp.2012.03.006

1251

1252 Lani, A., N. Villedieu, K. Bensassi, L. Kapa, M. Vymazal, M.S. Yalim, M. Panesi. COOLFluid: an open  
1253 computational platform for multi-physics simulation. Proc. 21st AIAA CFD Conference, *AIAA* **2013**-2589, San  
1254 Diego, June 2013, DOI: 10.2514/6.2013-2589

1255  
1256 Lakka, A., T.I. Pulkkinen, A.P. Dimmock, E. Kilpua, M. Ala-Lahti, I. Honkonen, M. Palmroth, and O.  
1257 Raukunen. GUMICS-4 analysis of interplanetary coronal mass ejection impact on Earth during low and  
1258 typical Mach number solar winds. *Ann. Geophys.*, **37**, 561–579, 2019, DOI: 10.5194/angeo-37-561-2019  
1259  
1260 Millward, G.H., R. J. Moffett, S. Quegan, and T. J. Fuller-Rowell. A coupled thermosphere ionosphere  
1261 plasmasphere Model (CTIP). STEP Handbook on Ionospheric Models, edited by R. W. Schunk, pp. 239–279,  
1262 Utah State Univ., Logan, 1996.  
1263  
1264 Newell, P.T, T. Sotirelis, K. Liou, and F.J. Rich. Pairs of solar wind-magnetosphere coupling functions:  
1265 Combining a merging term with a viscous term works best. *Journal of Geophysical Research: Space Physics*,  
1266 **113**, A04218, 2008, DOI: 10.1029/2007JA012825  
1267  
1268 O'Brien, T.P. and R.L. McPherron. An empirical phase space analysis of ring current dynamics: Solar wind  
1269 control of injection and decay. *J. Geophys. Res.*, **105**, 7707–7720, 2000, DOI: 10.1029/1998JA000437  
1270  
1271 Pomoell, J. and S. Poedts. EUHFORIA: European Heliospheric FORecasting Information Asset. *J. of Space*  
1272 *Weather and Space Climate*, **8**, A35, 2018, DOI: 10.1051/swsc/2018020  
1273  
1274 Scolini, C., C. Verbeke, S. Poedts, E. Chané, J. Pomoell, and F.P. Zuccarello. Effect of the initial shape of Coronal  
1275 Mass Ejections on 3D MHD simulations and geoeffectiveness predictions. *Space Weather*, **16**, 754–771, 2018,  
1276 DOI: 10.1029/2018SW001806  
1277  
1278 Taktakishvili, A., M. Kuznetsova, P. MacNeice, M. Hesse, L. Rastätter, A. Pulkkinen, A. Chulaki, D. Odstrcil.  
1279 Validation of the coronal mass ejection predictions at the Earth orbit estimated by ENLIL heliosphere cone  
1280 model. *Space Weather*, **7**, S03004, 2009, DOI: 10.1029/2008SW000448  
1281  
1282 Tóth, G., I.V. Sokolov, T.I. Gombosi, D.R. Chesney, C.R. Clauer, D.L. De Zeeuw, K.C. Hansen, K.J. Kane, W.B.  
1283 Manchester, R.C. Oehmke, K.G. Powell, A.J. Ridley, I.I. Roussev, Q.F. Stout, O. Volberg, R.A. Wolf, S. Sazykin,  
1284 A. Chan, B. Yu, J. Kóta. Space Weather Modeling Framework: A New Tool for the Space Science Community.  
1285 *Journal of Geophysical Research*, **110**, A12226, 2005, DOI: 10.1029/2005JA011126  
1286  
1287 Xia, C., J. Teunissen, I. El Mellah, E. Chané, and R. Keppens. MPI-AMRVAC 2.0 for solar and astrophysical  
1288 applications. *ApJ Suppl.*, **234**, 30 (26 pp), 2018, DOI: 10.3847/1538-4365/aaa6c8  
1289  
1290 Yalim M.S., and S. Poedts. 3D Global Magnetohydrodynamic Simulations of the Solar Wind/Earth's  
1291 Magnetosphere Interaction. in 'Numerical modeling of space plasma flows, ASTRONUM-2013', Proc. 8th  
1292 International Conference on Numerical Modeling of Space Plasma Flows (Astronom 2013), N.V. Pogorelov, E.  
1293 Audit, G.P. Zank (Eds.), July 1-5, 2013, Biarritz, FRANCE. ASP Conference Series, **488**, 192 -197, 2014.  
1294